Pesticide Biochemistry and Physiology 194 (2023) 105486

Contents lists available at ScienceDirect

Pesticide Biochemistry and Physiology

journal homepage: www.elsevier.com/locate/pest

# Biologically synthesized zinc and copper oxide nanoparticles using *Cannabis sativa* L. enhance soybean (*Glycine* max) defense against *fusarium virguliforme*

Ines Karmous [a,b,c,1,*], Shital Vaidya [a,1], Christian Dimkpa [a], Nubia Zuverza-Mena [a], Washington da Silva [a], Karol Alves Barroso [a], Juliana Milagres [a], Anuja Bharadwaj [a], Wael Abdelraheem [d], Jason C. White [a], Wade H. Elmer [a]

[a] The Connecticut Agricultural Experiment Station (CAES), CT, USA
[b] The Higher Institute of Applied Biology of Medenine (ISBAM), University of Gabes, Tunisia
[c] Faculty of Sciences of Bizerte (FSB), University of Carthage, Tunisia
[d] Centers for Disease Control and Prevention (CDC/NIOSH/HELD/CBMB), Ohio, USA

ARTICLE INFO

*Keywords:*
Antifungal
Biopesticide
*Cannabis sativa* L.
Copper oxide nanoparticles
*Fusarium virguliforme*
Zinc oxide nanoparticles

ABSTRACT

In this study, zinc and copper oxide nanoparticles (NPs) were synthesized using hemp (*Cannabis sativa* L.) leaves (ZnONP-HL and CuONP-HL), and their antifungal potential was assessed against *Fusarium virguliforme* in soybean (*Glycine* max L.). Hemp was selected because it is known to contain large quantities of secondary metabolites that can potentially enhance the reactivity of NPs through surface property modification. Synthesizing NPs with biologically derived materials allows to avoid the use of harsh and expensive synthetic reducing and capping agents. The ZnONP-HL and CuONP-HL showed average grain/crystallite size of 13.51 nm and 7.36 nm, respectively. The biologically synthesized NPs compared well with their chemically synthesized counterparts (ZnONP chem, and CuONP chem; 18.75 nm and 10.05 nm, respectively), confirming the stabilizing role of hemp-derived biomolecules. Analysis of the hemp leaf extract and functional groups that were associated with ZnONP-HL and CuONP-HL confirmed the presence of terpenes, flavonoids, and phenolic compounds. Biosynthesized NPs were applied on soybeans as bio-nano-fungicides against *F. virguliforme* via foliar treatments. ZnONP-HL and CuONP-HL at 200 μg/mL significantly ($p < 0.05$) increased (~ 50%) soybean growth, compared to diseased controls. The NPs improved the nutrient (e.g., K, Ca, P) content and enhanced photosynthetic indicators of the plants by 100–200%. A 300% increase in the expression of soybean pathogenesis related GmPR genes encoding antifungal and defense proteins confirmed that the biosynthesized NPs enhanced disease resistance against the fungal phytopathogen. The findings from this study provide novel evidence of systemic suppression of fungal disease by nanobiopesticides, via promoting plant defense mechanisms.

## 1. Introduction

The application of nanotechnology in agriculture has shown tremendous potential to overcome environmental challenges such as crop disease. Nanoparticles (NPs) consist of particles with dimensions between 1 and 100 nm (Vert et al., 2012). They can be natural or manufactured and include materials such carbon nanotubes, metallic NPs, metalloid NPs, and polymer-based NPs. Metal and metal oxide NPs have been incorporated into fertilizers and pesticides to promote plant health and crop growth (Dimkpa et al., 2012; Ishaq et al., 2019). Zinc oxide nanoparticles (ZnONP) have been studied in terms of their behavior in soil and potential effects on plants and food production (Sheteiwy et al., 2021). Copper oxide nanoparticles (CuONP) are known to be antimicrobial and insecticidal agents, along with being used as

* Corresponding author.
*E-mail addresses:* ineskarmouss@gmail.com (I. Karmous), shitalravaidya@gmail.com (S. Vaidya), Christian.Dimkpa@ct.gov (C. Dimkpa), Nubia.Zuverza@ct.gov (N. Zuverza-Mena), Washington.daSilva@ct.gov (W. da Silva), k.alvesbarroso@gmail.com (K.A. Barroso), juliana.s.milagres@ufv.br (J. Milagres), Anuja.Bharadwaj@ct.gov (A. Bharadwaj), whafez2008@gmail.com (W. Abdelraheem), Jason.White@ct.gov (J.C. White), wade.elmer@ct.gov (W.H. Elmer).
[1] Equal contribution of co-authors.

https://doi.org/10.1016/j.pestbp.2023.105486
Received 20 April 2023; Received in revised form 25 May 2023; Accepted 31 May 2023
Available online 5 June 2023

fertilizers (Dimkpa et al., 2012). Both ZnONP and CuONP improve soil fertility and provide important nutrients for enhancing plant development under environmental stress conditions (Karmous et al., 2022a, 2022b; Safa Hidouri et al., 2022), as well as provide protection against plant pathogens (Rossi et al., 2018). The efficiency of NPs has been attributed to their larger surface area and greater reactivity when compared to their equivalent bulk material, and are still influenced by the physicochemical properties of NPs, such as the size, charge, and morphology that are a function of synthesis conditions (Rastogi et al., 2017).

The synthesis of NPs includes various chemical methods, such as sol-gel, hydrothermal, spray pyrolysis, chemical vapor deposition, ultrasonic, precipitation, and microwave-assisted techniques (Abirami et al., 2020; Ijaz et al., 2020; Omri et al., 2014; Wang et al., 2010). However, many of these methods require high energy demand and may employ toxic and hazardous chemicals that compromise sustainability and lead to biological risk. Accordingly, biosynthesis of NPs, using biological systems has been explored as an alternative to conventional chemical and physical processes, as it is often a single-step, clean, safe, cost-effective and scalable process of producing NPs (Sharma et al., 2019). Plants also offer important advantages over other biological systems for NP synthesis, since plants are readily available, biochemically diverse, safe to handle, and the biosynthesized NPs are often more stable than chemically synthesized pristine analogs (Iravani, 2011). Plant extracts include natural compounds, secondary metabolites, and phyto-compounds that can effectively reduce, stabilize, and serve as capping agents in the NP biosynthesis process. The biosynthesis of zinc-based NPs has been carried out using different plants species, such as *Cassia fistula* L., *Trifolium pratenese* L., *Ocimum basilicum* L., *Melia azedarach* L, and *Ceratonia siliqua* L. (Naseer et al., 2020; Ramesh et al., 2015; Karmous et al., 2022a, 2022b). Copper-based NPs have also been biosynthesized from *Celastrus paniculatus* L. (Mali et al., 2020), and *Abies spectabilis* L. (Liu et al., 2020). Considerable effort has been devoted to screening different plant species for optimum use in NPs synthesis. Importantly, one of the goals of this effort is to develop novel natural fungicides as alternatives to existing synthetic formulations that often result in phytotoxicity, pest resistance, resurgence, vertebrate toxicity, widespread environmental hazards, and are expensive to produce (Zubrod et al., 2019).

Crop disease is a major factor threatening food security worldwide. Plant pathogens reduce global agricultural productivity by 20%, resulting in billions of dollars of annual losses (Savary et al., 2019). Crop diseases caused by pathogens such as viruses, bacteria, fungi, and nematodes not only decrease yield but also compromise produce quality and shelf life. Control efforts for fungal pathogens alone exceed $600 million per year and mycotoxin contamination impacts up to 25% of food crops globally (Eskola et al., 2020). For example, *Fusarium virguliforme* (Hartman et al., 2015) causes Sudden Death Syndrome (SDS) to soybean (*Glycine* max L.) and is widespread in the United States, causing $3.06 billion in annual losses. *F. virguliforme* resides in the soil, infects roots, colonizes xylem and phloem vascular elements, and is transported to aerial parts of the plant; colonization of the vasculature restricts water and nutrient flow in infected plants. The main symptoms of *Fusarium* infection include poor root development, foliar chlorosis, necrosis, and defoliation. The pathogen also compromises photosynthesis, and plant growth and yield, often leading to rapid mortality. SDS management has been difficult, although crop rotation and improved soil drainage offer some benefits; treating plants with ZnONPs and CuONPs may offer another strategy to manage this disease.

Evidence has shown that hemp (*Cannabis sativa* L.) extract exhibits antimicrobial activities (Khan, 2020; Schofs et al., 2021). *C. sativa* L. has received increased interest in the US due to recent regulatory changes that enable widespread cultivation. Hemp is a fast-growing plant that requires very little water and relatively few, if any, pesticides or synthetic fertilizers (Gill et al., 2022). The industrial use of hemp is gaining interest, especially in the western world, as it possesses several advantages in producing fabrics, clothing, and pharmaceuticals (Bridgeman and Abazia, 2017; Zimniewska et al., 2021).

The present study aimed to investigate the use of ZnONP and CuONP, either biologically synthesized from *C. sativa* or through a conventional chemical synthesis, to promote growth and control fungal disease in soybean. A special interest will be addressed to the physiological response of diseased soybean plants to the treatments with bio-NPs. Our working hypotheses were: (1) The leaf extract of *C. sativa* (HL) can be used in the biosynthesis of ZnONP and CuONP; (2) The biologically synthesized ZnONP-HL and CuONP-HL will display different physico-chemical properties, compared with chemically synthesized ZnONP and CuONP; (3) The application of ZnONP-HL and CuONP-HL will improve soybean growth and defense against *F. virguliforme* when compared to ZnONP chem and CuONP chem; and (4) The direct antifungal effects on the pathogen and/or the protective effects of NPs on soybean health will triggered by several physiological pathways, including (i) At the nutritional level, via the interference with the mineral balance and plant nutrition; and (ii) At the molecular level, via the modulation of pathogenesis-related genes (PR1a, PR2, and PR10). This study highlights the sustainable use of biosynthesized micronutrient nanomaterials as a key novel strategy to manage crop disease.

## 2. Materials and methods

### 2.1. Chemicals, Reagents, and biological materials

Zinc acetate dihydrate [Zn(CH3COO)2 · 2H2O] and copper (II) acetate monohydrate [$Cu(OOCCH_3)_2.H_2O$] were used for synthesis of the NPs. Soybean (*Glycine* max L.) seeds were purchased from Seed Ranch: Seed World USA, Odessa FL. Hemp (*Cannabis sativa* L.) Var Cherry Wine was cultivated at CAES according to Connecticut regulations for hemp cultivation.

### 2.2. Biosynthesis of ZnONP and CuONP from hemp extract

Hemp leaves (HL) from hemp variety Cherry Wine were dried in oven at 40 °C. Dried biomass (2 g) was ground to a fine powder, mixed in 200 mL of milli-Q water, and heated at 70 °C for 1 h under continuous shaking at 150 rpm. The homogenate was filtered three times through Whatman number-1 filter paper, and the filtrate was stored at 4 °C, for further use. For the preparation of ZnONP and CuONP, HL aqueous extract (50 mL) was added to equal volumes of 0.05 M Zinc acetate or 0.2 M Copper acetate. The pH of the mixture was adjusted to 12 for Zn-based NPs, and 8 for Cu-based NPs, by dropwise addition of 1 N NaOH. The mixture was then stirred for 1 h at 80 °C. The formation of ZnONP and CuONP was observed by development of a light-yellow color and a blue dark color, respectively. The precipitates were purified by centrifugation at 20000 ×*g* for 10 min with two subsequent washes with deionized water. Pellets were dried overnight in an oven at 60 °C, and the obtained powder materials are hereafter referred to as: "ZnONP-HL" and "CuONP-HL". The annotation "NPs-HL" refers to both ZnONP-HL and CuONP-HL. For the chemical synthesis of ZnONP and CuONP, 20 mL of milliQ water was mixed with 20 mL of zinc acetate or copper acetate solution, and then the process was conducted as described in the biosynthesis procedure, omitting HL extract (Lanje et al., 2010; Romadhan et al., 2016). The obtained nanoproducts were referred as: "ZnONP chem" and "CuONP chem" and the term "chem" refers to chemical synthesis without HL.

### 2.3. Characterization of NP

The optical properties of the NP were characterized using a Spectra Max M2 spectrophotometer. The crystallinity of the NPs was determined using a Rigaku Smart Lab X-Ray diffractometer (XRD), operating at 40 kV and 44 mA, and Cu Kα wavelength at 1.54060 A° (IRTracer-100 Shimadzu). Fourier Transform Infrared Spectrophotometry (FTIR) was

used to detect the presence of surface bonds for the bio-synthesized NPs at the wavelength of 400–4000 $cm^{-1}$, and a resolution of 2 $cm^{-1}$. Dynamic light-scattering (DLS) was used to determine the particle size distribution and zeta potential, which represents the charge on the NPs' surface. Transmission electron microscopy (TEM) images was used to characterize particle morphology and size (Hitachi HT 7800, 120 kV).

### 2.4. Qualitative and quantitative analysis of the hemp extract

Five grams of hemp leaves were dried at 40 °C, ground in a mortar and then 50 mL of absolute methanol was added. Then the mixture was kept under continuous shaking overnight. The mixture was then centrifuged at 10000 x*g* for 10 min. The supernatant was filtered using a microfilter of 0.2 μm, and the obtained filtrate was analyzed by gas chromatography with mass spectrometry (GC–MS).

Analysis was performed using Agilent 7890B-GC with Agilent 5977A MSD. A splitless injection of volume of 0.8 μL was used at an inlet temp of 325 °C, and a flow 60 mL/min with an inlet liner (Supelco cup design with glass wool packing). The initial oven temperature was 80 °C, ramp 1 of hold time 0 min, ramp 1 = 5 °C/min to 120 °C, ramp 2 = 10 °C/min to 280 °C with a hold time of 4 min thus total run time of 28 min. The column used was Agilent 19091S-433 HP-5MS Phenyl Methyl Silox, 29.72 m × 0.25 mm × 0.25 μm. A Helium carrier gas was used. The instrument conditions were as follows: MSD-heater set to 280 °C, Tune File – Atune, Ionization: Positive Electron Impact, Acquisition mode – Scan, MS Quad – 150 °C, MS Source temperature 230 °C, Low Mass – 70, High Mass – 500, Threshold – 100, Solvent Delay – 1.0 min Transfer line temperature 250 °C, Electron Energy: 70 V.

### 2.5. Inoculum preparation

The *Fusarium virguliforme* (FUS) inoculum was prepared as previously described (Elmer and White, 2014; Peréz et al., 2020). Briefly, three colonized PDA agar plugs (4 mm diam.) were seeded into flasks filled with autoclaved Japanese millet, allowed to grow for 2 weeks at 22–25 °C, air dried in paper bags, and then ground into a powder in a coffee mill. The inoculum concentration was a 2 g/L soilless potting mix (ProMix BX, Premier Hort Tech).

### 2.6. Greenhouse experiment

The soybean cultivar 'Seedranch' (SeedRanks, Inc.) was used to evaluate the capacity of ZnONP-HL and CuONP-HL to induce disease suppression. Soybean seeds were inoculated with *Rhizobium* prior to seedling by soaking in soybean inoculant (active ingredient: *Bradyrhizobium japonicum* 4%, 2.1 fl.oz./140Kunit of seed). The soybean seeds were germinated in 36 cell trays 5.8 × 4.9 × 5.6 cm filled with soilless potting mix (ProMix BX, Premier Brand Inc., New Rochelle, NY) and fertilized once after three weeks with Miracle Gro soluble 24–8-16 (N-P-K) fertilizer (Scotts Miracle grow Marysville MD). When plants reached the 3- to 4-leaf stage, medium size plants were selected and transplanted into a FUS-amended potting mix (FUS treatment) or in a potting mix without FUS (Pathogen-free controls). During this transfer, transplants were 10 days-old. Foliar application of ZnONP-HL, CuONP-HL, ZnONP chem, and CuONP chem was carried out using a "plant dip" procedure, allowing a complete immersion of leaves (duration of 1 min for each plant for each treatment). The ZnONP chem and CuONP chem treatments served as a reference to determine mechanistic differences in bioactivity based on the synthesis method. Prior to amendment, the NP suspensions were sonicated using a bath sonicator for 30 min. The plants across all treatments were foliar treated with the NP suspensions two times (days 10 and 11). In each treatment, 10 biological replicates (1 plant/pot) were included. As part of a pre-screening experiment, the NPs were used at 100, 200, 400 and 500 mg/L. The concentration of 200 mg/L was then selected as the dose allowing both improvement of plant growth and the recovery/defense against FUS infection. All plants were maintained under greenhouse conditions (temperature, 25 °C; relative humidity, 74%; light period, 16/8, day/night), and irrigated with tap water daily for 30 days. At harvest, root and shoot length, root fresh biomass, and fresh biomass of shoot and leaves were measured across all the treatments. Fresh samples (leaves, roots, and shoots) were stored at −80 °C for gene expression analysis; additional samples were dried in an oven at 60 °C for 3 days and used to determine dry biomass and element content.

### 2.7. Photosynthesis measurement

Prior to harvest, the photosynthetic efficiency of the treated soybean leaves was measured. A leaf in the same position on each seedling was selected for analysis by a portable Photosynthesis System (LI-COR Biosciences). Per instrument conditions, the $CO_2$ in the reference chamber was fixed at 400 μmol $mol^{-1}$, the relative humidity was between 50 and 65%, the light intensity was 750 μmol $m^{-2}$ $s^{-1}$ and the flow was 200 μmol $s^{-1}$. The instrument was recalibrated every 15 samples to obtain stable readings. Parameters measured were: Phi2: % light to photochemistry; PhiNPQ: % light to non-photochemical quenching; Phi NO: % light to other; relative chlorophyll content; ECSt: difference in protonmotive force from light (max) to dark (min); VH+: flow rate of H+ through ATP synthase; $gH^+$: permeability of thylakoid membrane; PAR: light intensity, photosynthetically active radiation; Leaf angle: angle of leaf relative to the ground; and Leaf temperature differential: difference of temperature between the leaf and ambient air.

### 2.8. Measurement of minerals

Dry soybean shoots and roots (300 mg) were separately ground into fine powders in a mill and digested using 3 mL of 70% $HNO_3$ with heating at 115 °C for 45 min on a heating block (DigiPREP System; SCP Science). The digested samples were cooled down to room temperature, and total volume was adjusted to 50 mL by adding deionized water. The content of minerals, including Zn and Cu, was measured using inductively coupled plasma optical emission spectroscopy (iCAP 6000; DAC0083, Thermo Fisher Scientific). Individual elemental concentrations were calculated as mg $kg^{-1}$ dry biomass.

### 2.9. Gene expression analysis

Total RNA was extracted from treated plant samples by first grinding 100 mg of fresh leaves in liquid nitrogen, followed by use of the Pure Link Plant RNA Reagent (Thermo Fisher Scientific, Waltham, MA-USA) following the manufacturer's recommendations. The RNA concentration was measured with a Nanodrop 2000 Spectrophotometer (Thermo Fisher Scientific, Waltham, MA-USA), and RNA integrity was verified on 1% agarose gel electrophoresis. The RNA was then treated with TURBO Dnase-free (Thermo Fisher Scientific, Waltham, MA-USA,) to remove residual DNA. First-strand cDNA was synthesized using SuperScript™ III Reverse Transcriptase kit (Thermo Fisher Scientific, Waltham, MA-USA). Quantitative PCR (qPCR) was performed on the cDNA samples using SsoAdvanced™ Universal SYBR® Green Supermix kit (Bio-Rad Laboratories, Inc., Hercules, CA-USA). The PCR was run at 95 °C for 30 s, followed by 39 PCR cycles (95 °C for 30 s, then 60 °C for 30 s, 65 °C for 5 s, and final extension at 95 °C for 5 s) on a Bio-Rad CFX96 thermocycler (Bio-Rad Laboratories, Inc., Hercules, CA-USA). The Melt curve was at 65 °C and the analysis of qPCR data was performed using the $2^{-\Delta\Delta Ct}$ method, and GmEF1b was the housekeeping gene. The relative fold change of each gene was expressed as $\log_2$ ($2^{-\Delta\Delta Ct}$). The targeted fragments of GmPR1a (155 bp), GmPR2 (165 bp), and GmPR10 (127 bp) genes were amplified using the following primers: for gene GmPR1a, primers GmPR1a-F (TGA AAA TGT GGG TTG ATG AGA AAT) and GmPR1a-R (AAG TGA TGA AAG TGC CTC CGT T); for gene GmPR2, primers GmPR2-F (GTT CGG AAT GTG AAG CAA GGA) and GmPR2-R: (ATA GGA GAA AAG AGC CGC CAA); and for gene GmPR10, primers

GmPR10-F: (TAG CAT CCA CAG CAT TGT TTT C) and GmPR10-R: (CAA GGC AGT GCC CTC AGT TA). The house-keeping gene (GmEF1b) primers used were GmEF1b-F: (CCA CTG CTG AAG AAG ATG ATG ATG) and GmEF1b-R (AAG GAC AGA AGA CTT GCC ACT C). The GenBank accession number of the studied genes are GmPR1a (AF136636), GmPR2 (M37753), GmPR10 (FJ960440). The housekeeping gene - GmEF1b GenBank accession no. is NM_001248778.

### 2.10. Statistical analysis

The greenhouse trials were arranged in a randomized complete block design (RCBD) with ten biological replicates. All data were subjected to analysis of variance (ANOVA) using 'SPSS Statistics version 20' software. The treatments were considered as main factors. Means comparisons were performed using ANOVA at $\alpha = 0.05\%$, and Post Hoc test of Duncan multi-range test at 5%.

## 3. Results and discussion

### 3.1. Physicochemical properties of the nanoparticles

The UV–vis absorption spectra of biologically and chemically synthesized NPs are shown in Fig. 1A and B. The biosynthesized ZnO nanoparticles show an absorption peak at 350 nm, whereas chemically synthesized ZnO nanoparticles have a maximum absorption peak at 360 nm. This shows that the band gap increases with decreasing particle size (Bhuyan et al., 2015). More specifically, the blue shift of absorption for the biosynthesized "ZnONP-HL" in comparison with chemically synthesized "ZnONP chem" is likely due to the decrease in particle size, which is consistence with other studies (Inamdar et al., 2014; Segets et al., 2009). Similarly, "CuONP-HL" and "CuONP chem" showed a broad absorption peak at 370 nm, which agrees with other reports (Naika et al., 2015). This indicates a possible element-specific influence of hemp-derived capping molecules and related changes in molecular orbitals. Notably, there was some pH dependence as well as the reactions were more effective at pH 12 for ZnONP and pH 8 for CuONP (data not shown). The particles were further characterized by XRD analysis. ZnONP-HL and ZnONP chem showed a diffraction pattern in accordance with the standard peaks displayed by the International Centre for Diffraction Data card no. 01–080-0075, which confirms the hexagonal wurtzite structure for the synthesized ZnONP. The average grain/crystallite size of NP from the highest intense peak (101) was calculated using the Debye–Scherer eq. (1). The calculated average grain size was 13.51 nm for "ZnONP-HL", 18.75 nm for "ZnONP chem", 7.36 nm for "CuONP-HL", and 10.05 nm for "CuONP chem". This difference between NPs synthesized with and without leaf extract suggests that certain components of the hemp extract act as capping agents to stabilize the NPs, which agrees that biosynthetic routes provide NPs of better-defined sizes and morphology as compared to other physicochemical methods (Raveendran et al., 2003) who reported. Similarly, CuO-HL and CuO chem showed diffraction peaks that correspond to copper oxide ICCD card no. 01–089-5898. Interestingly, ZnONP chem and CuONP chem both showed sharp diffraction peaks, compared to ZnONP-HL and CuONP-HL, suggesting smaller particle size of the biosynthesized NPs (Fig. 1C, D).

FTIR analysis allows us to ascertain the purity and chemical nature of the NPs, as well as the presence of phytochemicals and functional groups in the HL extract. Phytochemicals such as flavones, alcohols, phenols, amines, carboxylic acids, sugars, and ketones can interact with the particle surface, and aid in the stabilization of ZnONP-HL and CuONP-HL, which prevents further growth and agglomeration of NPs (Ovais et al., 2018; Pradeep et al., 2022). The hemp's phytochemicals playing the role of the capping agents of the NPs were analyzed by FTIR spectroscopy (Niraimathi et al., 2013; Prakash et al., 2013). The FTIR spectra showed peaks at the range of 400–4000 $cm^{-1}$ at a resolution of 2 $cm^{-1}$ (Fig. 1E, F). Metal oxides generally show absorption peaks in the regions between 600 and 400 $cm^{-1}$ (Nayan et al., 2019). The comparison between the FTIR spectra of ZnONP-HL, ZnONP chem, CuONP-HL, and CuONP chem against the NP-free HL extract revealed similar stretching vibrations, confirming that several phytocompounds of HL were serving

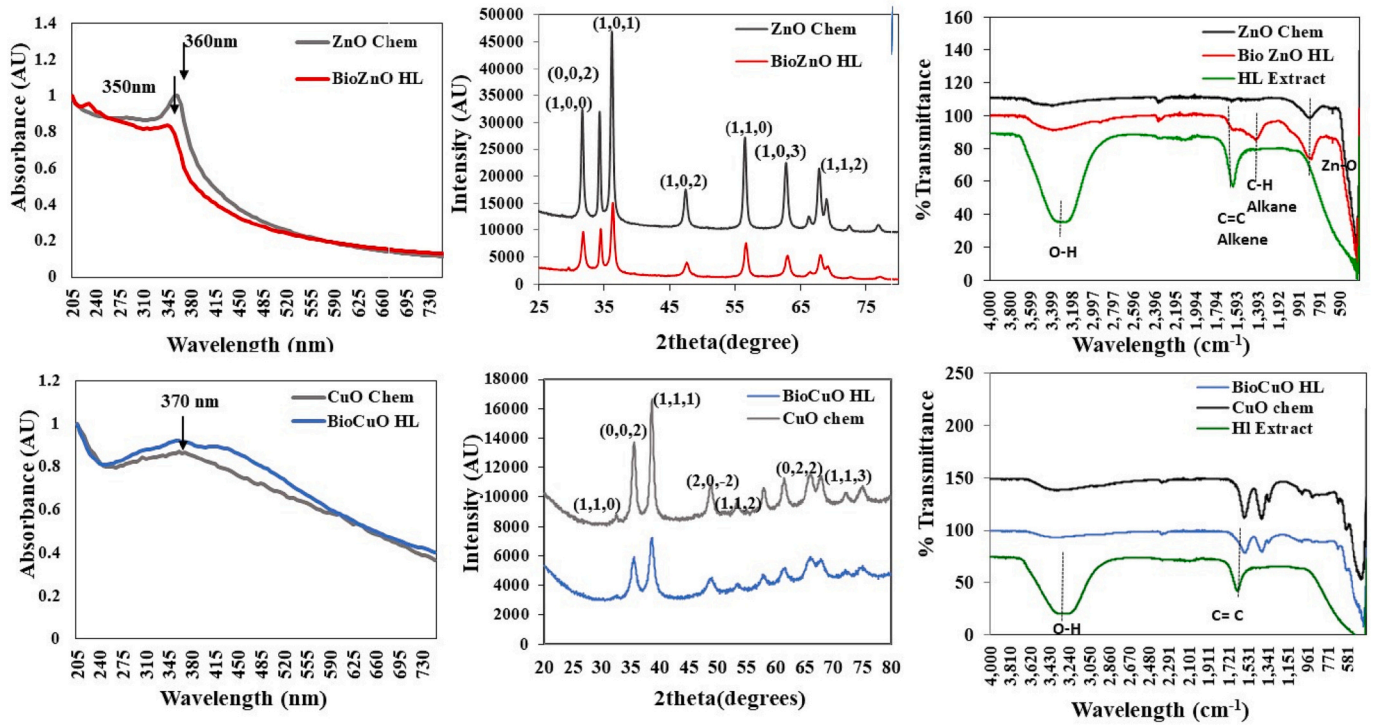


**Fig. 1.** Properties of ZnONP-HL, CuONP-HL, ZnONP-chem, and CuONP-chem with UV–vis spectroscopy (A, B), X-Ray Diffraction (XRD) (C, D), and Fourier Transform Infrared Spectroscopy (FTIR) (E, F).

as coating and stabilizing agents for ZnONP-HL and CuONP-HL. For instance, the hemp leaf extract showed absorption peaks at 3300 $cm^{-1}$ and 1650 $cm^{-1}$, which corresponds to O-H (water) and C═C (alkene) stretches, respectively. In addition, at peak for ZnONP-HL was evident at 1668 $cm^{-1}$, which indicates the influence of alkene (C═C) stretching on ZnO surface bonds. This weak stretch recorded at 1668 $cm^{-1}$ might be due to the formation of surface bonds between ZnO and alkenes from HL extract. The peak that was observed for ZnONP-HL at 960 $cm^{-1}$ corresponds to Zn—O tetrahedral bond formation. The Zn—O frequencies observed for the synthesized ZnONP are in accordance with values in the literature (Brügel, 1965; Singh et al., 2011). The FTIR spectrum of CuONP-HL depicted distinctive characteristic bands at 1630–1740 $cm^{-1}$, 1650 $cm^{-1}$, 1437 $cm^{-1}$, and 1550–1500 $cm^{-1}$, which correspond to C═O stretching, C═C stretching, O—H stretching, and N═O stretching, respectively. The peaks at 3300 $cm^{-1}$ and 1650 $cm^{-1}$ corresponded to the hemp leaf extract bands. These peaks indicate the presence of terpenes, flavonoids, and phenolic compounds in the HL extract. The presence of terpenes in the hemp leaf extract was also confirmed by GC–MS analysis. The presence of alkene bonds in the hemp leaf extract and corresponding deviations in ZnONP-HL and CuONP-HL indicated the influence of terpene on the surface of the biosynthesized nanoparticles. These phytochemicals also stabilize NPs by chelating with metal ions through carbonyl groups or p-electrons. These findings demonstrate that the surface of hemp-mediated ZnONP-HL and CuONP-HL were capped with and stabilized by phytochemicals from the hemp leaf extract, including terpenes.

DLS analysis was used to determine particle hydrodynamic diameter and zeta potential was measured to indicate electrical charge. ZnONP-HL showed a negative zeta potential at −18.35 mV and an average diameter of 259.5 nm, while ZnONP chem showed a positive charge of +18.72 mV and an average particle diameter of 224.6 nm (Table S1). The negative zeta potential of ZnONP-HL indicates strong repellent force among the particles that minimizes agglomeration. CuONP-HL and CuONP chem had zeta potentials of +22.37 mV and + 31.62 mV, respectively, and hydrodynamic diameters of 242.9 nm and 235.8 nm, respectively (Table S1). However, for better determination of particle size, the NPs were further analyzed by TEM.

Fig. 2 shows TEM images of ZnONP-HL, CuONP-HL, ZnONP chem, and CuONP chem. The average size of nanoparticles calculated by Image J software was 57.39 nm for ZnONP-HL (Fig. 2A) and 99.71 nm for ZnONP chem (Fig. 2B). For CuONP-HL (Fig. 2C), the TEM image showed there was agglomeration (average size 122.71 nm) of small nanoparticles (average size 10.59 nm). Conversely, CuONP chem (Fig. 2D) showed only larger clusters of an average size of 137 nm. TEM analysis confirms the role of biomolecules as capping agents, leading to the formation of smaller-size nanoparticles with biosynthesis as compared to conventional chemical synthesis.

The analysis of hemp leaf extract by GC–MS revealed a range of compounds commonly associated with this species, including tetrahydrocannabinol (THC), cannabidiol (CBD), cannabigerol (CBG), cannabinol (CBN), (−)-Δ8-transtetrahydrocannabinol (Δ8-THC), cannabicyclol (CBL), cannabinodiol (CBND), cannabielsoin (CBE), and cannabitriol (CBT) (data not shown). In this study, however, the focus was on phenolic acids, flavonoids, and terpenes that may play a role in

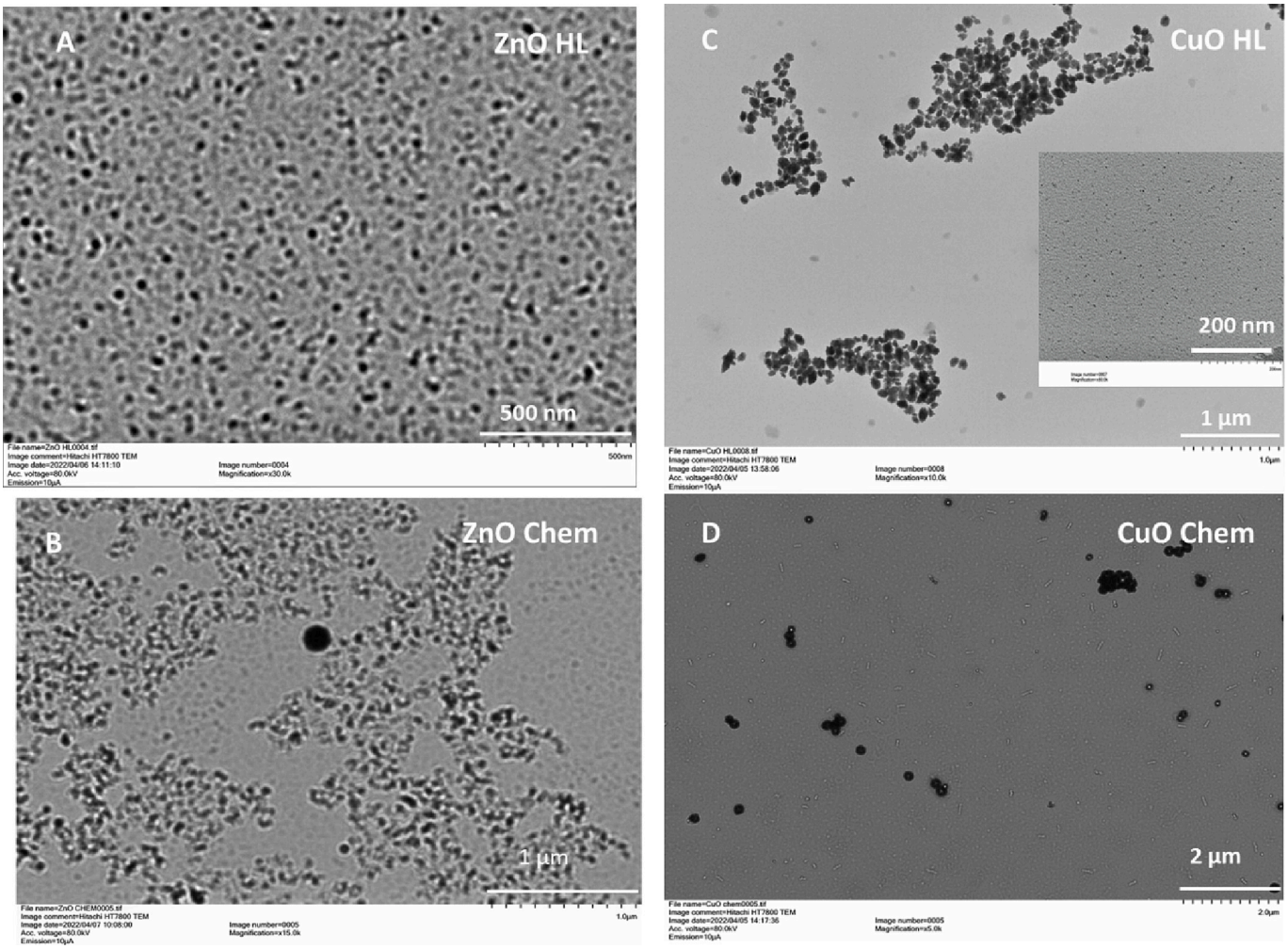


**Fig. 2.** Transmission Electron Microscopy (TEM) images of ZnONP-HL, CuONP-HL, ZnONP-chem, and CuONP-chem.

reducing Zn and Cu ions, stabilizing and capping the NPs during synthesis (Table S1). In general, numerous phytochemicals were detected (see full list in Table S1); the main bioactive secondary metabolites consist of terpenes and terpenoids, as well as sesqui-, mono-, di-, and triterpenoids, such as trans-caryophyllene, γ-selinene, alpha-humulene, 2-naphthalenemethanol, and benzene. These metabolites may become incorporated during the nanoparticle biosynthesis process, conveying unique properties to biologically synthesized NPs.

### 3.2. Effect of NP on growth of soybean infected with FUS

Soybean plants grown in infested soil showed a highly significant ($p < 0.001$) inhibition of shoot growth starting from day 22, reaching an approximately 50% decreased by day 27 when compared to healthy controls (Figs. 3). Compared the healthy controls, plants in infested soil had a 50% reduction in both the length of the internodes (Fig. 4A) and the number of leaves (Fig. 4C). In addition, fresh shoot biomass (Fig. 5B), root length and biomass (Figs. 5D, E), and the fresh and dry biomass of leaves (Figs. 5C, 6C) were all significantly ($p < 0.05$) decreased in the infested plants. Similarly, a 70% reduction in root biomass and length was evident in the diseased plants (Figs. 5, 6A). Importantly, the FUS-induced damage was significantly ($p < 0.001$) alleviated by the foliar application of biosynthesized ZnONP-HL and CuONP-HL at concentrations of 100 mg/L and 200 mg/L, respectively (Fig. 3A, B). At day 27, the shoot length was indeed improved by around 30% and 50%, with ZnONP-HL and CuONP-HL, respectively, compared to FUS-infested plants (Fig. 3A, B). Also, healthy plants showed a highly significant increase ($p < 0.001$) of shoot length on days 20 and 22, respectively, with 100, 200 and 400 mg/L ZnONP-HL, as compared to control plants (Fig. 3C). CuONP-HL showed a significant increase ($p <$

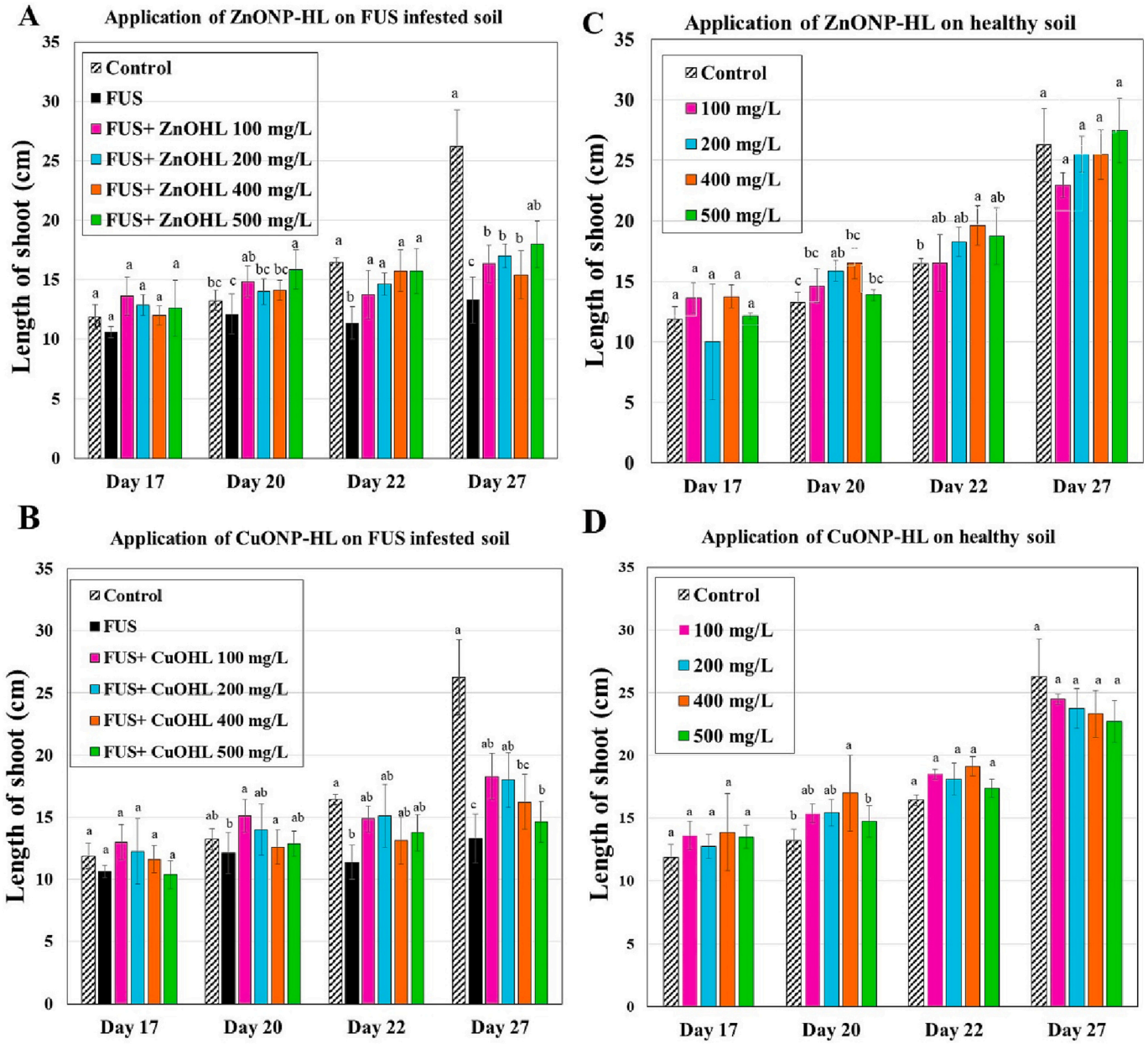


**Fig. 3.** Screening the effects of different concentrations of ZnONP-HL (A, C) and CuONP-HL (B, D) on the shoot length of soybean plants grown on FUS infested soil (A, B). Controls were cultivated on healthy soil (C, D). Plants were treated with 100, 200, 400 and 500 mg/L ZnONP-HL or CuONP-HL. Data are Means ±SD resulting from 10 biological replicates, and whole experiments were technically repeated 3 times. The significance of the difference between treatments was determined by ANOVA ($\alpha = 0.05$) was evaluated at $p < 0.001$. Letters denote statistical differences between treatments using the Duncan test ($\alpha = 0.05$).

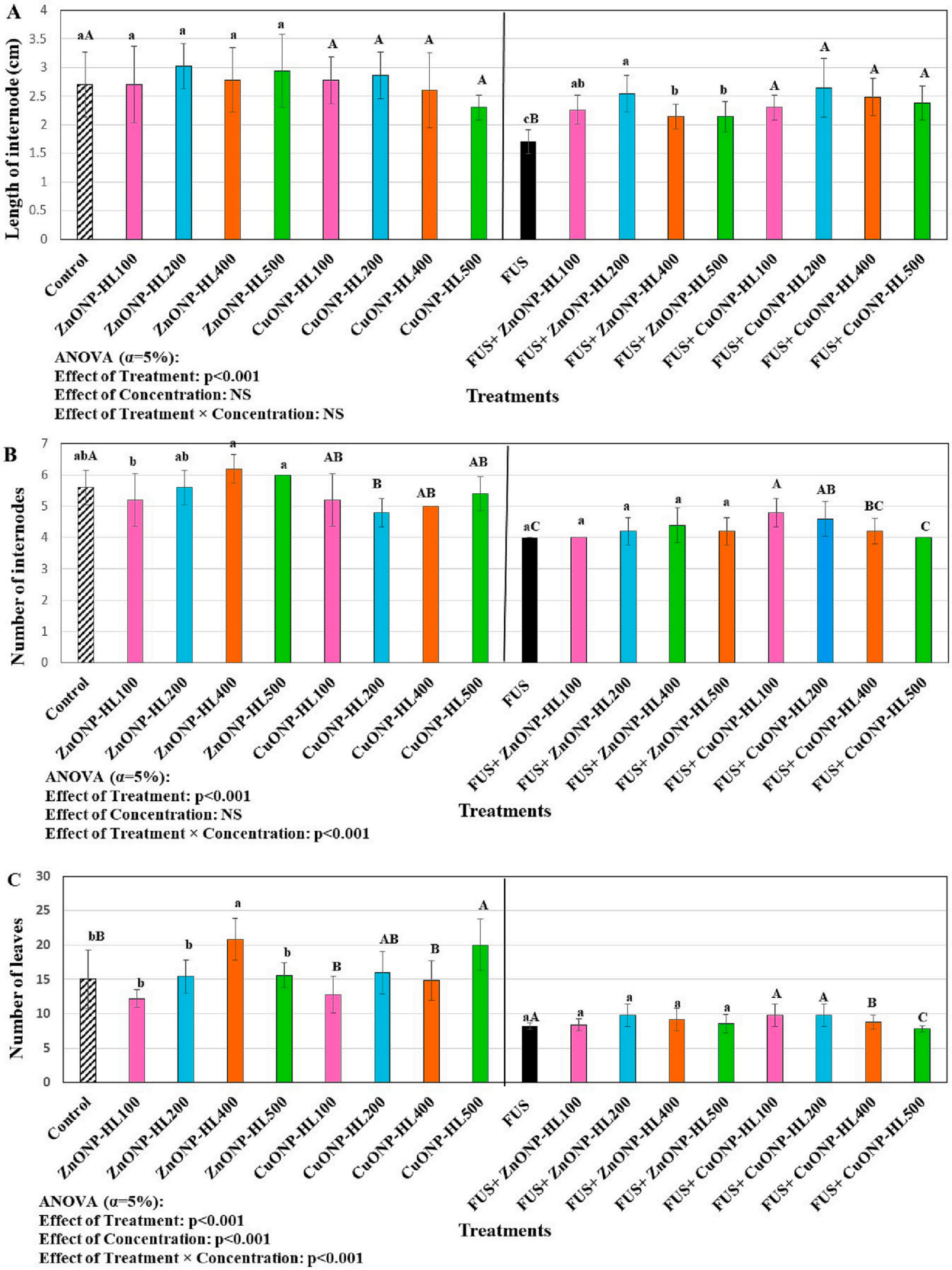


**Fig. 4.** Screening the effects of different concentrations of ZnONP-HL and CuONP-HL on the length of internode (A), number of internodes (B), and number of leaves (C) of soybean plants cultivated on control soil or soil infested with FUS. Plants were treated with 100, 200, 400 and 500 mg/L ZnONP-HL or CuONP-HL. Data are Means ±SD resulting from 10 biological replicates, and whole experiments were technically repeated 3 times. The significance of the difference between treatments was determined using ANOVA (α = 0.05) was evaluated at $p < 0.05$. Letters (a-c) and (A-C) denote statistical differences, respectively, between control and ZnONP-HL treatments, and between control and CuONP-HL, using the Duncan test (α = 0.05).

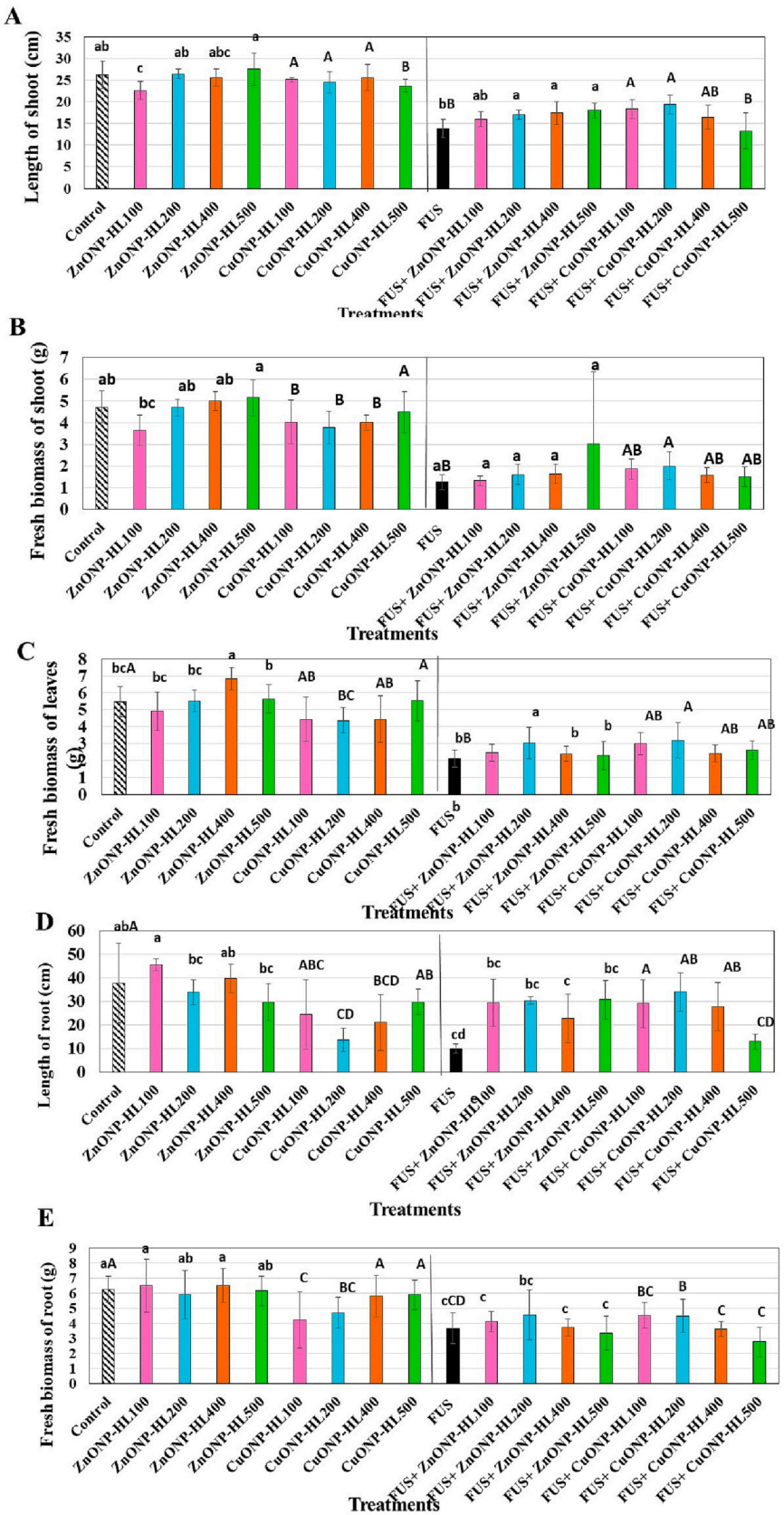


**Fig. 5.** Screening the effects of different concentrations of ZnONP-HL and CuONP-HL on the shoot length (A), shoot fresh biomass (B), leaf fresh biomass of leaves (C), length of root (D), and fresh biomass of root (E) of soybean plants cultivated on control soil or soil infested with FUS. Plants were treated with 100, 200, 400 and 500 mg/L ZnONP-HL or CuONP-HL. Data is Means ±SD resulting from 10 biological replicates, and whole experiments were technically repeated 3 times. The significance of the difference between treatments was determined using ANOVA ($\alpha = 0.05$) was evaluated at $p < 0.05$. Letters (a-c) and (A-C) denote statistical differences, respectively, between control and ZnONP-HL treatments, and between control and CuONP-HL, using the Duncan test ($\alpha = 0.05$).

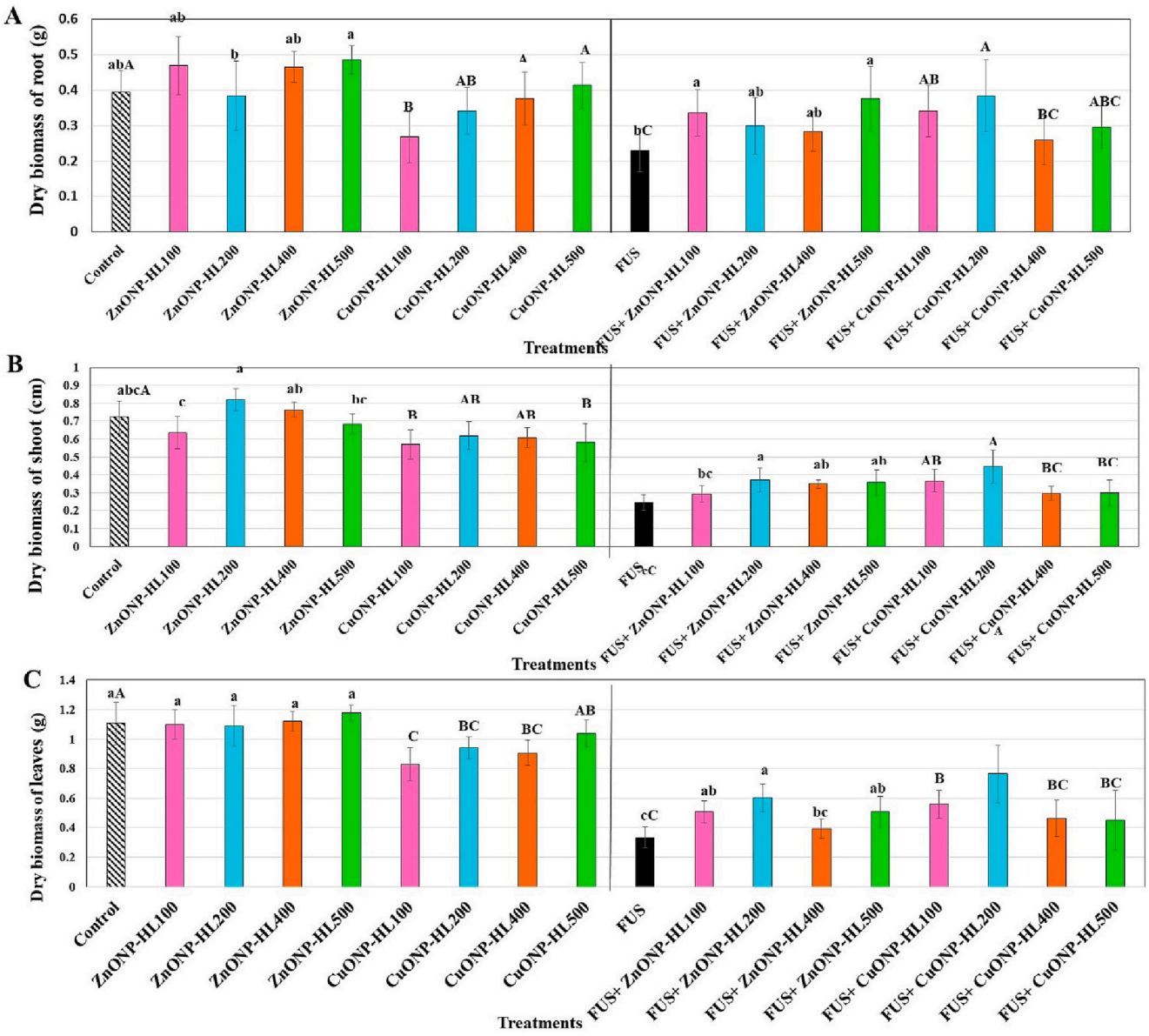


**Fig. 6.** Screening the effects of different concentrations of ZnONP-HL and CuONP-HL on the root dry biomass (A), shoot dry biomass (B), and leaf dry biomass (C) of soybean plants, cultivated on control soil or soil infested with FUS. Plants were treated with 100, 200, 400 and 500 mg/L ZnONP-HL or CuONP-HL. Data are Means ±SD resulting from 10 biological replicates, and whole experiments were technically repeated 3 times. The significance of the difference between treatments was determined using ANOVA ($\alpha = 0.05$) was evaluated at $p < 0.05$. Letters (a-c) and (A-C) denote statistical differences, respectively, between control and ZnONP-HL treatments, and between control and CuONP-HL, using the Duncan test ($\alpha = 0.05$).

0.001) of the shoot length at day 20 with concentrations of 100, 200 and 400 mg/L (Fig. 3D) in comparison to control plants, while no significant improvement was found at days 22 and 27.

The response of soybean to NP application differed in control versus FUS infested condition. In FUS infested soil, ZnONP-HL and CuONP-HL significantly ($p < 0.05$) increased the shoot length compared with the disease control (Fig. 3, 5A), particularly at 100 and 200 mg/L. ZnONP-HL and CuONP-HL had no significant effect on the length of internode under control condition, but increased significantly ($p < 0.05$) the length of internode of FUS-infested plants and treated with NPs, especially with 100 and 200 mg/L (Fig. 4A). The number of internodes showed no variation with the treatment FUS + ZnONP-HL, while the treatment FUS + CuONP-HL had an increasing effect on this endpoint (Fig. 4B). Similarly, ZnONP-HL and CuONP-HL did not affect positively the number of leaves of FUS-stressed plants (Fig. 4C). On the other hand, ZnONP-HL increased fresh leaf biomass (Fig. 5C), root length (Fig. 6A), and the fresh root biomass (Fig. 6B), particularly at 100 and 200 mg/L, compared with FUS infested controls. CuONP-HL also increased shoot length and fresh biomass by 50% as compared with FUS-infected plants (Fig. 5A, B). Similarly, dry shoot biomass increased by 20% with ZnONP-HL 200 and 400 mg/L, and nearly 100% with CuONP-HL at 200 mg/L (Fig. 6B). Additionally, CuONP-HL increased leaf growth and fresh biomass by 50% and 25% as compared with FUS-stressed plants (Fig. 5C). This recovery was more evident in dry leaf biomass, which increased by approximately 200% with CuONP-HL as compared to FUS infested controls (Fig. 6C). In addition, both ZnONP-HL and CuONP-HL alleviated the disease induced inhibition of root elongation (Fig. 5A), fresh biomass (Fig. 5B), and dry biomass (Fig. 6A). More specifically, 100–200 mg/L ZnONP-HL and 200 mg/L CuONP-HL induced a 3.0- and 3.5-times increase in root length, respectively (Fig. 5D). The root dry biomass was also increased by 200 mg/L ZnONP-HL (around 100%) and CuONP-HL (200%) (Fig. 6C). The concentrations of 400 mg/L and 500

mg/L resulted in either no significant change in plant endpoints or effects that were significantly ($p < 0.05$) less than that of 100 and 200 mg/L.

Importantly, 200 mg/L was the most effective dose for alleviation FUS damage on soybean. For instance, ZnONP-HL and CuONP-HL led to recovery of shoot growth (around 40% increase) and fresh and dry biomass (around 60% increase) compared to the untreated controls (Figs. 7, 8). Moreover, both NP treatments resulted in a >200% increase in root length. Similarly, ZnONP-HL and CuONP-HL increased the fresh and dry biomass by 20% and 40% compared with disease controls, respectively (Figs. 7, 8). The leaf dry biomass was increased by approximately 57%, although the impact of fresh leaf biomass was not statistically significant (Fig. 8). These findings are in line with other studies that showed the ameliorating effects of ZnONP and CuONP on coffee (*Coffea arabica* L.) (Rossi et al., 2018) and grass pea (*Lathyrus sativus* L.) (Arfaoui et al., 2021) when these plants were subjected to adverse environmental conditions. These findings are in accordance with other studies showing that biologically synthesized NPs are a promising alternative to conventionally synthesized materials and are biocompatible, efficient, non-toxic, and eco-friendly NPs (Parveen et al., 2016; Patil and Chandrasekaran, 2020).

In a case of study, the concentration 20 μg/mL ZnONPs enhanced *Brassica junca* seed germination and plant height, however, 30 μg/mL or higher concentration showed significant ($p < 0.05$) decrease in seed

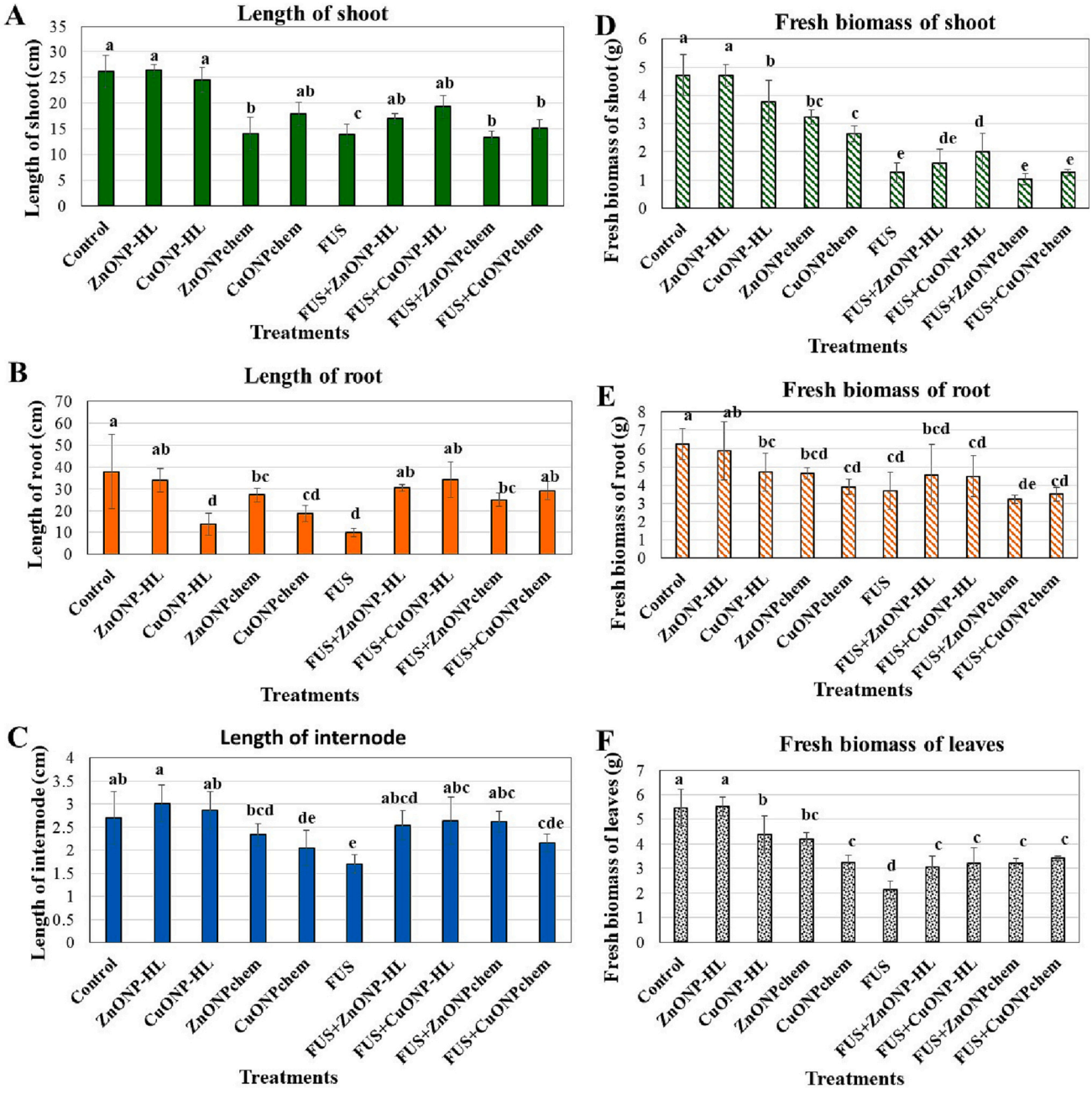


**Fig. 7.** Growth parameters of soybean plants cultivated on control soil or soil infected with FUS for 30 days; shoot length (A), root length (B), internodes length (C), fresh shoot biomass (D), fresh root biomass (E), and fresh leaf biomass (F). Plants were treated with 200 mg/L ZnONP-HL, CuONP-HL, ZnONP-chem, and CuONP-chem. Data are Means ±SD resulting from 10 biological replicates, and whole experiments were repeated 3 times. The significance of the difference between treatments was determined using ANOVA ($\alpha = 0.05$) was evaluated at $p < 0.05$. Letters denote statistical differences between treatments using the Duncan test ($\alpha = 0.05$).

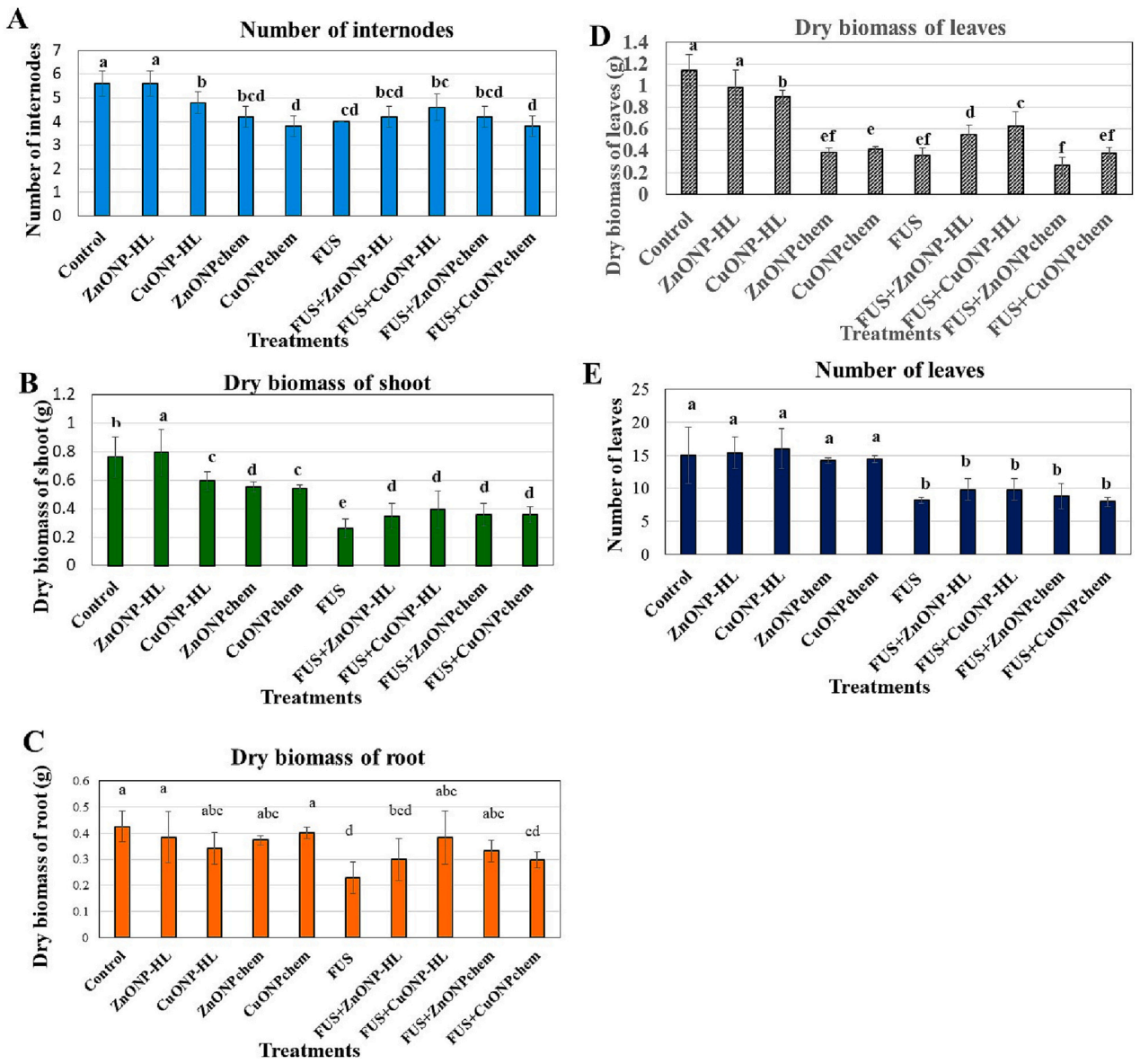


**Fig. 8.** Growth parameters of soybean plants cultivated on control soil or soil infected with FUS for 30 days; Number of internodes (A), dry shoot biomass (B), dry root biomass (C), dry leaf biomass (D), and number of leaves (E). Plants were treated with 200 mg/L ZnONP-HL, CuONP-HL, ZnONP-chem, and CuONP-chem. Data are Means ±SD resulting from 10 biological replicates, and whole experiments were repeated 3 times. The significance of the difference between treatments was determined using ANOVA ($\alpha = 0.05$) was evaluated at $p < 0.05$. Letters denote statistical differences between treatments using the Duncan test ($\alpha = 0.05$).

germination and plant height which indicating that ZnO NPs up to 20 μg/ml is beneficial for plant and can be used as fertilizers (Mazumder et al., 2020). Similarly, the reduction of dry biomass of *B. junca* plants was only 19% at 1 mg/L ZnONPs and it increased up to 63% at 20 mg/L ZnONPs (Zafar et al., 2016). In another study, chemically synthesized CuONPs decreased the germination rate and biomass or rice, while biologically synthesized CuONPs increased antioxidant activities and callogenesis (Anwaar et al., 2016; da Costa and Sharma, 2023).

### 3.3. Mechanism of action of ZnONP-HL and CuONP-HL against FUS

The relationship between the physiological growth of plants and mineral nutrition was further investigated to understand the mechanism of disease suppression. We hypothesized that fully understanding the state of mineral nutrition would provide insight on the role of NPs-HL in soybean defense against disease. This was tested by analyzing the elemental composition in the leaves (Fig. 9) and roots (Fig. 10) of the plants. Since we adopted the strategy of foliar application of NPs and roots are the target of FUS as a soilborne disease, this analysis may highlight the possible coordination between leaf and root response during pathogen invasion and plant response.

FUS differentially affected the elemental composition of soybean leaves and roots. In leaves, phosphorus (P) levels were decreased after exposure to FUS, while levels of other macronutrients and micronutrients were unaffected by FUS. Also, there was a decline of Na and Se content versus the increase of Ca, S, Mg, Cu, Zn, Fe, and B (Fig. 9). In roots, the levels of P, K, Zn and Si were decreased significantly ($p < 0.05$) as compared to the respective control values (Fig. 9). No significant variation was detected for other nutrients, including Mg, Ca, S, Cu, Co, Mn and Mo. Conversely, the root levels of Na, Fe, and Mo were increased (Fig. 10).

The subsequent application of ZnONP-HL on FUS-infested plants triggered qualitative and quantitative changes in the mineral content of the leaves. For instance, increases in the levels of Ca, K, S, and P suggests that ZnONP-HL alleviates the FUS-driven inhibition of P accumulation and also likely enhances the assimilation of Ca, K, S and P in the leaves

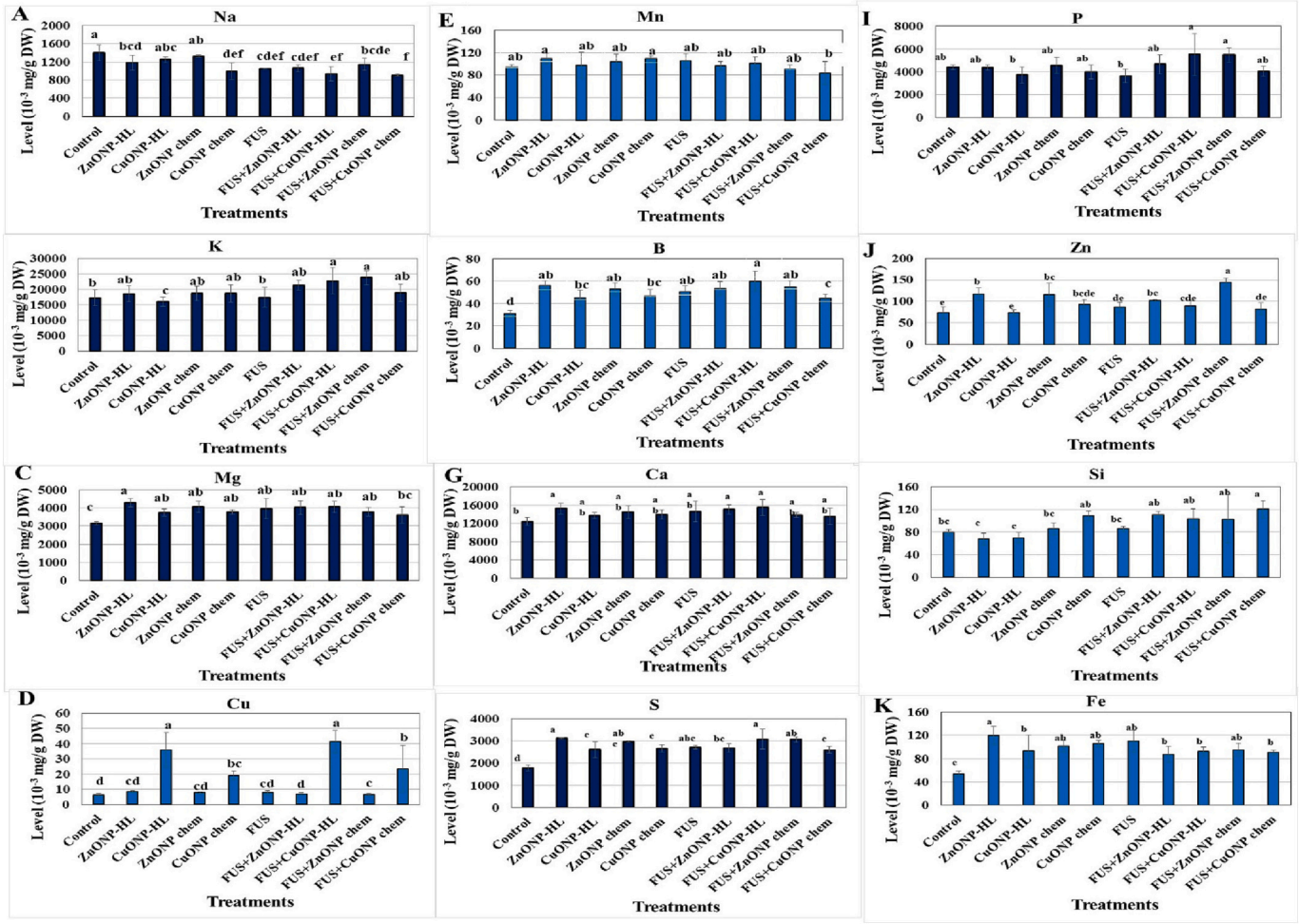


**Fig. 9.** Levels of nutrients in soybean leaves; Na (A), K (B), Mg (C), Cu (D), Mn (E), B (F), Ca (G), S (H), P (I), Zn (J), Si (K), and Fe (L). Plants were cultivated on control soil or soil infected with FUS for 30 days and were treated with 200 mg/L ZnONP-HL, CuONP-HL, ZnONP chem, and CuONP chem. Data are Means ±SD resulting from 3 biological replicates, and whole experiments were technically repeated 2 times. The significance of the difference between treatments was determined using ANOVA ($\alpha = 0.05$) was evaluated at $p < 0.05$. Letters denote statistical differences between treatments using the Duncan test ($\alpha = 0.05$).

(Fig. 9).

This finding was also evident with CuONP-HL for Ca content, as well with even greater levels K, S, and P showed higher levels (40, 20, and 35% respectively, compared to FUS). This may suggest enhanced availability/usage of K, S, and P with the application of CuONP-HL, as compared with ZnONP-HL (Fig. 9). In addition, Cu and Zn were obviously impacted by NP foliar application; Cu content increased by >300% with CuONP-HL, whereas Zn content was enhanced by 30% with ZnONP-HL treatment. In roots, ZnONP-HL and CuONP-HL similarly restored the levels of K and P (Fig. 10), suggesting improved absorption of these nutrients over the disease controls. ZnONP-HL also reduced the absorption of Na and enhanced the uptake of Ca by the roots (Fig. 10). There were no changes in the levels of Zn and Cu in roots upon foliar application of ZnONP-HL and CuONP-HL (Fig. 10). Conversely, the root content of other nutrients was enhanced by CuONP-HL, including Mn and Fe, or by both ZnONP-HL and CuONP-HL, in the case of Mo and Si. The nutritional status of plants is critical for tolerance to pathogenic attack. Thus, these changes in the macronutrient and micronutrient content may be a critical component by which NPs convey pathogen resistance or suppression in soybean. The recovery of the uptake of these essential minerals improves intracellular ionic homeostasis, and consequently, the synthesis of defense proteins, phytohormones, antioxidants, and signaling molecules.

Interestingly, the biologically synthesized and chemically synthesized NPs had different impacts on nutrient uptake. In the leaves of FUS exposed plants, ZnONP chem more effectively restored the levels of K, P, S, Zn, and Fe, compared with ZnONP-HL, while the later improved the Ca content more than did ZnONP chem. Furthermore, CuONP-HL was more efficient than CuONP chem at restoring the levels of Ca, K, S, P, Cu, Zn, Mn, and B in diseased plants. CuONP-HL seems to restore more Cu than CuONP chem, but for Zn, ZnONP chem resulted in more Zn than ZnONP-HL. The findings were different in the roots (Fig. 10), where ZnONP-HL and CuONP-HL were less efficient at facilitating the recovery of P, Zn, and Si than were the chemically synthesized particles. However, ZnONP-HL did increase Mg and Ca content. Furthermore, the comparison between the elemental composition in the shoot and root tissues suggests that ZnONP-HL and CuONP-HL differentially modulate nutrient uptake and translocation.

Importantly, FUS exposure increased the bioavailability of several non-essential elements in the leaves, such as Al, Ti, Pb, and As (Fig. S1), and similarly the uptake of Pb by the roots (Fig. S2). Nonetheless, the application of ZnONP-HL or CuONP-HL reduced the leaf content of Ti, Cd and As, and the root content of Ti and As (Figs. S1, S2). A number of photosynthetic parameters were measured as a function of disease and treatment (Table S3.1, S3.2). FUS-infected plants showed reduced NPQ, which was accompanied by an increased flow rate for protons ($VH^+$). The relative chlorophyll content was significantly ($p < 0.05$) reduced in plants infected with FUS, while the PS1 oxidized center activity increased significantly ($p < 0.05$), compared to controls. Importantly, relative chlorophyll content is one of the essential factors responsible for

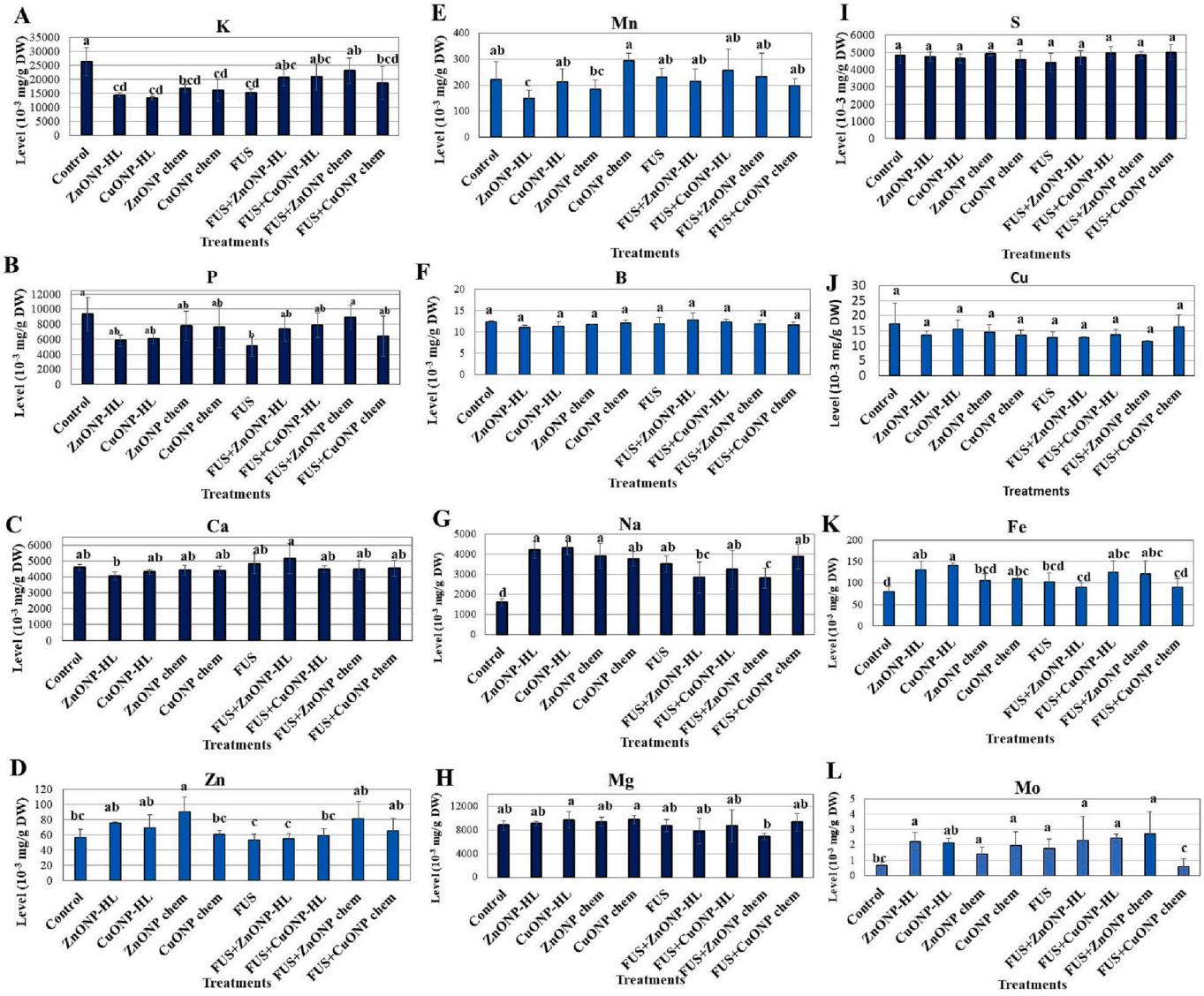


**Fig. 10.** Levels of macronutrients in soybean roots; K (A), P (B), Ca (C), Na (D), Mg ϵ, and S (F). Plants were cultivated on control soil or soil infected with FUS for 30 days and were treated with 200 mg/L ZnONP-HL, CuONP-HL, ZnONP chem, and CuONP chem. Data are Means ±SD resulting from 3 biological replicates, and whole experiments were technically repeated 2 times. The significance of the difference between treatments was determined using ANOVA ($\alpha = 0.05$) was evaluated at $p < 0.05$. Letters denote statistical differences between treatments using the Duncan test ($\alpha = 0.05$).

the efficient absorption of light ultimately leading to carbon fixation and agronomic yield. The findings from FUS-infected plants suggest the alteration of certain parameters (NPQt, PhiNPQ, PS1 open centers, and relative chlorophyll content), collectively resulting in reduced carbon fixation rates and slower biomass accumulation. However, the activation of other parameters ($VH^+$, LEF, PAR, and PS1 oxidized centers) suggests a photosynthetic induction, likely as part of a systemic effort to cope with the pathogen stress.

During photosynthesis, energy is transiently stored as an electrochemical proton gradient across the thylakoid membrane, thus resulting in a proton motive force that induces the synthesis of ATP. In our study, the flow rate of $H^+$ through ATP synthase ($VH^+$) increased with all treatments, in comparison to healthy control. The highest levels were recorded with FUS + CuONP chem (100% increase), FUS + CuONP-HL (60% increase), and ZnONP-HL (50% increase). Leaf angle relative to the ground did not change with "FUS" but decreased with the application of NPs-HL and NPs chem, as compared with controls, with FUS + ZnONP chem. Photosynthetically active radiation (PAR) increased significantly ($p < 0.05$) with FUS + CuONP chem, and with FUS, FUS + ZnONP chem, FUS + CuONP-HL, and FUS + ZnONP-HL. (Peng, 2000) reported the risk of photodamage under extremely high PAR, temperature extremes, and water deficit. By implication, increased PAR results in a decrease in light-harvesting efficiency and photosynthetic capacity, likely associated with a decrease in chlorophyll content. Conversely, the percentage of light energy captured by photosystem PSII (NPQt) decreased significantly ($p < 0.05$) with FUS, FUS + ZnONP chem, FUS + CuONP chem (Table S3.2), while less impact was evident with ZnONP-HL, ZnONP chem, and CuONP chem. CuONP-HL did not affect NPQt as compared to controls. No significant induction was observed for the percentage of light energy captured by PSII, light directed towards photochemistry (Phi2), or energy-dependent quenching, which is the main component of non-photochemical quenching (Phi NPQ). Similar results were found for PS1 active centers with all treatments (Table S3.2.). The application of ZnONP-HL or ZnONP chem did not restore PS1 to control levels, but CuONP-HL and CuONP chem did achieve this result. The PS1 seems to shift towards oxidation in healthy plants, but was reduced with ZnONP-HL, CuONP-HL, ZnONP chem, and CuONP chem. The application of NP-HL or NP-chem triggered numerous

changes in the levels of several photosynthetic parameters, including PAR, LEF, Phi2, PS1 oxidized centers, and relative chlorophyll content. Similar results were found when plants were infected with FUS and treated with NPs-HL or NPs chem (Table S3), which may be an in-planta response to meet metabolic needs by controlling photochemical reactions occurring in the chloroplast thylakoid membrane, the splitting of water into oxygen, the transfer of protons and electrons, and the production of energy molecules adenosine triphosphate (ATP) and nicotinamide–adenine dinucleotide phosphate (NADPH). Taken together, the data reveal differential effects of ZnONP-HL, CuONP-HL vs ZnONP chem, and CuONP chem on the photosynthesis parameters. Both ZnONP-HL and CuONP-HL tended to correct the relative chlorophyll induced by FUS (Table S3–2), while ZnONP-HL and CuONP-HL improved LEF and VH+, respectively (Table S3–1).

### *3.4. Effects of ZnONP-HL and CuONP-HL on soybean molecular response to FUS*

We speculate that the protective effects of NP-HL observed in our study derive from unique molecular signaling pathways involving enzymes and proteins associated with host defense responses under pathogen stress. To that end, we investigated the regulation of GmPR1a, GmPR2, and GmPR10 genes upon pathogen infection in the leaves of plants cultured under control, FUS, ZnONP-HL, CuONP-HL, FUS + ZnONP-HL, and FUS + CuONP-HL (Fig. 11, Fig. S3). We were interested in these PR genes because they encode PR pathogenesis-related proteins, which are generally produced in plants in the event of a pathogen attack. The level of expression of the GmPR1a gene was low in the control treatment but increased (up-regulation) with ZnONP-HL (Fig. 11A), thus suggesting that ZnONP-HL induced the expression of GmPR1a protein. However, GmPR1a expression was down-regulated in the presence of CuONP-HL, thus suggesting that CuONP-HL reduced the expression of GmPR1a protein. Under FUS stress, the expression of GmPR1a decreased. We hypothesize either; (i) plants were not able to activate GmPR1a gene expression under FUS stress, which suggests that this may not be involved in the defense response against this pathogen; or (ii) FUS may act by inhibiting GmPR1a gene expression, thus leading to decreased defense activity. Nonetheless, foliar application of ZnONP-HL and CuONP-HL on diseased plants was able to significantly ($p < 0.05$) induce GmPR1a gene expression; these findings align with the previous study of (Elmer et al., 2018).

The PR1a gene encodes PR1 protein involved in the salicylic acid (SA)-dependent pathway. SA is known for mediating host responses upon pathogen infection and can be negatively affected by pathogen effectors (Hao et al., 2018; Zhao et al. Adisa et al., 2019). In the current study, the decreased expression of GmPR1a gene with FUS infection suggests that the pathogen may have interfered with SA accumulation, disrupting SA signaling pathways, and compromise plant defense against pathogen (Lefevere et al., 2020). Thus, induction of GmPR1a upon application of ZnONP-HL and CuONP-HL to FUS infected plants may be linked to the activation of SA-mediated defense signaling pathways, which may result in decreased pathogen virulence or enhanced plant defense.

Another pathogenesis-related (PR) gene, GmPR2, was analyzed in this study (Fig. 10B). This gene encodes the PR-2 family of pathogenesis-related proteins known as β-1,3-glucanases (Balasubramanian et al., 2012), and defends plants against pathogen infection (Leubner-Metzger and Meins, 1999; Ruiz-Herrera and Ortiz-Castellanos, 2019). The upregulation of GmPR2 in FUS infected plants may suggest different metabolic pathways involving β-1,3-glucanases, such as their accumulation in the event of FUS pathogen attack, and the direct hydrolysis of β-1,3-glucans found in the walls of FUS. This finding suggests that differential expression of PR-2 β1,3-glucanases may be associated with increased disease resistance, which agrees with previous reports(Gupta et al., 2012; Perrot et al., 2022). Here, upregulation of GmPR2 in healthy plants treated with ZnONP-HL or CuONP-HL demonstrates the inducing

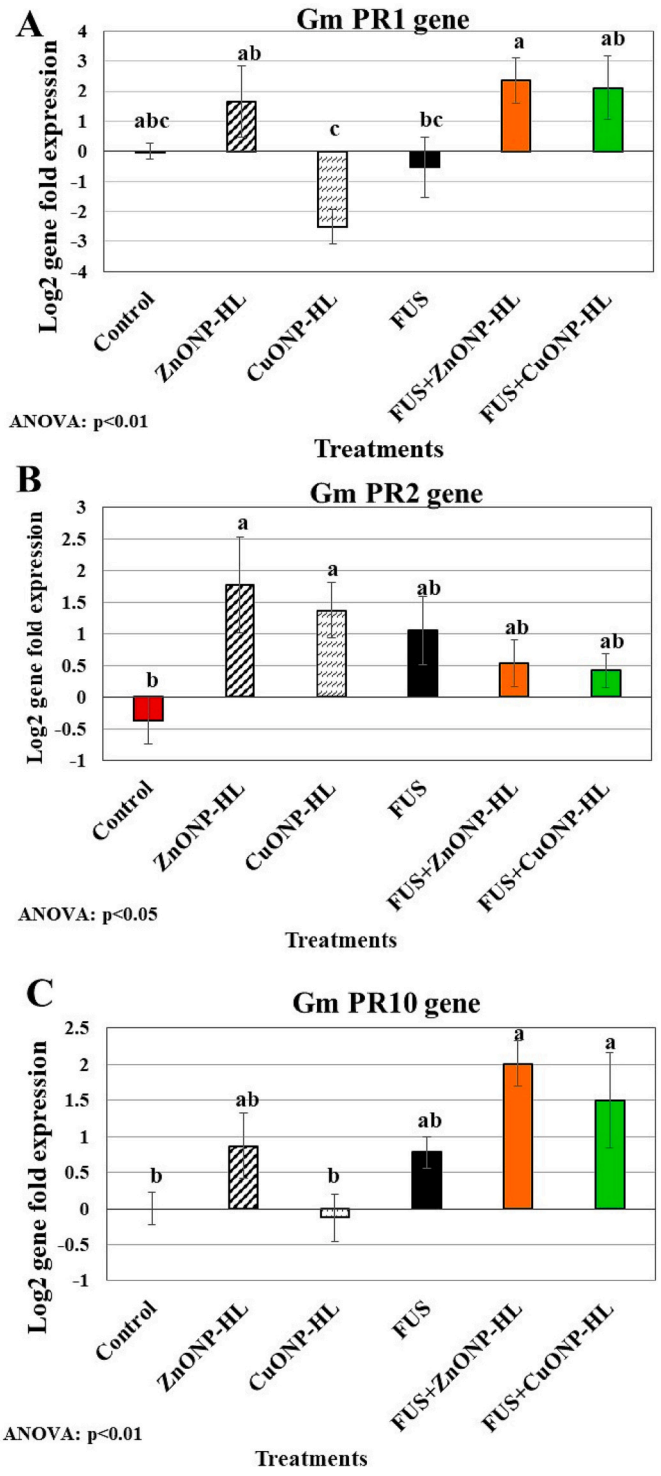


**Fig. 11.** Levels of expression of pathogen related genes by RT-qPCR in soybean leaves; Gm PR1 gene (A), Gm PR2 gene (B), and Gm PR10 gene (C). Plants were cultivated on control soil or soil infected with FUS for 30 days. Plants were treated with 200 mg/L ZnONP-HL, CuONP-HL, ZnONP chem, and CuONP chem. Data are Means ±SE resulting from at least 3 biological replicates, and whole experiments were technically repeated 5 times. The significance of the difference between treatments was determined using ANOVA ($\alpha = 0.05$) was evaluated at $p < 0.05$. Letters denote statistical differences between treatments using the Duncan test ($\alpha = 0.05$).

properties of NPs-HL. This finding suggests involvement of β-1,3-glucanases in soybean growth and development, likely by regulating the accumulation and degradation of callose deposits in the plasmodesmata (Pd). Interestingly, GmPR2 expression was downregulated in FUS-infected plants after the application of ZnONP-HL and CuONP-HL (Fig. 11B). This may be explained by the reduction of β-1,3-glucanases activity in the presence of FUS + NPs-HL. Therefore, the protective effects of ZnONP-HL and CuONP-HL on soybean against FUS either do not involve PR2 proteins, or alternatively, were efficient at FUS disease suppression, subsequently downregulating GmPR2 expression.

ZnONP-HL and CuONP-HL induced the expression of GmPR10 gene in FUS infected soybean (Fig. 11C). This suggests a significant ($p < 0.05$) role for GmPR-10 in the defense response against this pathogen. The highest levels of expression were detected with FUS, consistent with the colonization of the plant. The overexpression of GmPR10 was more significant ($p < 0.05$) when ZnONP-HL and CuONP-HL were applied to FUS diseased plants; there was a 2-fold increase of GmPR10 gene transcripts with FUS + ZnONP-HL and FUS + CuONP-HL compared to disease controls. This partly explains the greater disease resistance in "FUS + NPs-HL". This finding is in line with (Wu et al., 2016), where the overexpression of rice defense-related gene GmPR10 enhanced tolerance to pathogen infections and lead to differential modulation of various proteins related to oxidative stresses, carbohydrate metabolism, and plant defense. Similarly, PR-10 genes were upregulated after *Verticillium dahliaiae* infection of strawberry plants (Besbes et al., 2019). Additionally, (Li et al., 2021) conducted a gene expression analysis in *Panax notoginseng* and showed that PnPR-like was responsive to an infection by the root rot pathogen *Fusarium solani*. The authors demonstrated that the PnPR-like protein had antifungal effects in vitro on *F. solani* and *Colletotrichum gloeosporioides*. The accumulated PR proteins also help prevent reinfection through the development of systemic acquired resistance (Zhang et al., 2019).

Taken together, the expression analyses of GmPR1a, GmPR2, and GmPR10 suggests either their protective effects on plants or inhibiting effects on the FUS pathogen. This type of interaction involves complex functional relationships between plant defense genes and pathogens, which are interconnected into complex defense networks, and requires in-depth molecular level studies to fully understand the mechanisms involved. The application of ZnONP-HL and CuONP-HL may actively inhibit FUS on soybean through PR defense signaling networks, which in turn restrict the further growth and spread of the pathogen. Importantly, the NPs-HL induced differential responses of PR genes involved in a number of pathways, leading to interconnecting pathways that orchestrate the control of plant defense. The increased expression of PR genes with "FUS + NPs-HL" were measured in non-infected leaves of the host, as a soilborne disease FUS targets mainly roots. Therefore, NPs-HL seems to activate the systemic acquired resistance (SAR) pathway, which agrees with reports by (Ali et al., 2018).

## 4. Conclusions

This study contributes novel insights into our understanding of soybean response to *Fusarium* pathogen, as well as provides important information towards the development of practical, efficient and safe strategies using biologically synthesized NPs from hemp to promote resistance to FUS stress. ZnONP-HL and CuONP-HL demonstrated a marked efficacy in promoting the physiological functions in soybean plants, despite infection with *Fusarium*. NPs-HL were able to activate different strategies in soybean to fight off the fungal pathogen, such as recovery of essential nutrients in roots and leaves, and the induction of PR genes. This may ensure a further activation of defense signal pathways and a production of antifungal compounds like PR proteins, which further restricts pathogen invasion. Overall, the biologically synthesized NPs may trigger a higher potential in promoting plant growth and disease suppression, compared to the chemically synthesized counterparts. Nonetheless, it is apparent that more research is needed to further elucidate the effect of biologically synthesized NPs on plant defense systems. Additionally, biologically synthesized NPs need to be investigated on different crops to unravel their positive and negative effects on agricultural systems. More understanding of the insights into the molecular mechanisms of the interaction between NPs and plants should be explored at several aspects, such as the molecular signaling pathways, secondary metabolites, and the defense genes response. A fine tuning of the of biosynthesized NPs technologies might therefore help in the management of plant diseases of global importance.

### Ethics approval/declarations

Not applicable.

### Consent to participate

Not applicable.

### Consent for publication

Not applicable.

### Code availability

Not applicable.

### CRediT authorship contribution statement

**Ines Karmous:** Conceptualization, Investigation, Methodology, Data curation, Formal analysis, Funding acquisition, Validation, Writing – original draft, Writing – review & editing. **Shital Vaidya:** Investigation, Methodology, Data curation, Formal analysis, Writing – original draft, Writing – review & editing. **Christian Dimkpa:** Conceptualization, Resources, Funding acquisition, Validation, Writing – review & editing. **Nubia Zuverza-Mena:** Methodology, Resources, Formal analysis, Writing – review & editing. **Washington da Silva:** Methodology, Resources, Data curation, Formal analysis, Funding acquisition, Validation, Writing – review & editing. **Karol Alves Barroso:** Methodology, Data curation. **Juliana Milagres:** Methodology, Data curation. **Anuja Bharadwaj:** Methodology, Writing – review & editing. **Wael Abdelraheem:** Methodology. **Jason C. White:** Resources, Funding acquisition, Validation, Writing – review & editing. **Wade H. Elmer:** Conceptualization, Resources, Funding acquisition, Validation, Writing – review & editing.

### Declaration of Competing Interest

None.

### Data availability

The datasets generated during and/or analyzed during the current study are available from the corresponding author on reasonable request.

### Acknowledgments

Thanking is addressed to the grant of Fulbright in Tunisia-USA (2021−2022). We thank Mrs. Regan Huntley (CAES) for her assistance and help in purchasing materials and chemicals, and Ms. Terri Arsenault (CAES) for kindly providing the hemp material. We also acknowledge the help of Dr. Fabian Menges (Yale University) with the FTIR analyses. We thank Dr. Min Li for providing access to Yale west campus materials characterization core facility.

## Appendix A. Supplementary data

Supplementary data to this article can be found online at https://doi.org/10.1016/j.pestbp.2023.105486.

## References


Abirami, N., Arulmozhi, R., Siddharth, A.G.S., 2020. Plant mediated synthesis, characterization of zinc oxide nanoparticles using *simarouba glauca* and its antibacterial activities. Res. J. Pharm. Technol. 13, 1817–1822. https://doi.org/10.5958/0974-360X.2020.00327.3.

Adisa, Ishaq O., Dimkpa, Christian O., Jorge, L., Gardea-Torresdey, White, Jason C., 2019. Recent advances in nano-enabled fertilizers and pesticides: a critical review of mechanisms of action. Environ. Sci. Nano 6, 2002.

Ali, S., Ganai, B.A., Kamili, A.N., Bhat, A.A., Mir, Z.A., Bhat, J.A., Tyagi, A., Islam, S.T., Mushtaq, M., Yadav, P., Rawat, S., Grover, A., 2018. Pathogenesis-related proteins and peptides as promising tools for engineering plants with multiple stress tolerance. Microbiol. Res. 212–213, 29–37. https://doi.org/10.1016/J.MICRES.2018.04.008.

Anwaar, S., Maqbool, Q., Jabeen, N., Nazar, M., Abbas, F., Nawaz, B., Hussain, T., Hussain, S.Z., 2016. The effect of green synthesized CuO nanoparticles on callogenesis and regeneration of *Oryza sativa* L. Front. Plant Sci. 7, 1330. https://doi.org/10.3389/FPLS.2016.01330/BIBTEX.

Arfaoui, H., Karmous, I., Mahjoubi, Y., Kharbech, O., Tlahig, S., Loumerem, M., 2021. Screening of the effects of zinc oxide based nanofertilizers on the germination of *Lathyrus sativa* L. seeds. J. Appl. Bot. Food Qual. 94, 53–60. https://doi.org/10.5073/JABFQ.2021.094.007.

Balasubramanian, V., Divya Cletus, J., Sakthivel, N., 2012. Plant b-1,3-glucanases: their biological functions and transgenic expression against phytopathogenic fungi. https://doi.org/10.1007/s10529-012-1012-6.

Besbes, F., Habegger, R., Schwab, W., 2019. Induction of PR-10 genes and metabolites in strawberry plants in response to *Verticillium dahliae* infection. BMC Plant Biol. 19, 1–17. https://doi.org/10.1186/S12870-019-1718-X.

Bhuyan, T., Mishra, K., Khanuja, M., Prasad, R., Varma, A., 2015. Biosynthesis of zinc oxide nanoparticles from *Azadirachta indica* for antibacterial and photocatalytic applications. https://doi.org/10.1016/j.mssp.2014.12.053.

Bridgeman, M.B., Abazia, D.T., 2017. Medicinal Cannabis: history, pharmacology, and implications for the *acute care* setting. Pharm. Therapeut. 42, 180.

Brügel, W., 1965. Chemical applications of infrared spectroscopy. Von C. N. R. Rao. Academic press, New York-London 1963. 1. Aufl., XIII, 683 S., zahlr. Abb. u. Tab., geb. $ 19.50. Angew. Chem. 77, 391. https://doi.org/10.1002/ANGE.19650770833.

da Costa, M.V.J., Sharma, P.K., 2023. Effect of copper oxide nanoparticles on growth, morphology, photosynthesis, and antioxidant response in *Oryza sativa*. https://doi.org/10.1007/s11099-015-0167-5.

Dimkpa, C.O., McLean, J.E., Britt, D.W., Anderson, A.J., 2012. Bioactivity and biomodification of ag, ZnO, and CuO nanoparticles with relevance to plant performance in agriculture. Ind. Biotechnol. 8, 344–357. Doi: https://doi.org/10.1089/IND.2012.0028/ASSET/IMAGES/LARGE/FIGURE5.JPEG.

Elmer, W.H., White, J.C., 2014. Environmental Science Nano PAPER The use of metallic oxide nanoparticles to enhance growth of tomatoes and eggplants in disease infested soil or soilless medium. https://doi.org/10.1039/c6en00146g.

Elmer, W., Majumdar, Sanghamitra, Zuverza-Mena, N., 2018. Effect of Metalloid and Metal Oxide Nanoparticles on Fusarium Wilt of Watermelon. https://doi.org/10.1094/PDIS-10-17-1621-RE.

Eskola, M., Kos, G., Elliott, C.T., Hajšlová, J., Mayar, S., Krska, R., 2020. Worldwide contamination of food-crops with mycotoxins: validity of the widely cited 'FAO estimate' of 25%. Crit. Rev. Food Sci. Nutr. 60, 2773–2789. https://doi.org/10.1080/10408398.2019.1658570.

Gill, A.R., Loveys, B.R., Cowley, J.M., Hall, T., Cavagnaro, T.R., Burton, R.A., 2022. Physiological and morphological responses of industrial hemp (*Cannabis sativa* L.) to water deficit. Ind crops. Prod 187, 115331. https://doi.org/10.1016/J.INDCROP.2022.115331.

Gupta, P., Ravi, I., Sharma, V., 2012. Induction of β-1,3-glucanase and chitinase activity in the defense response of *Eruca sativa* plants against the fungal pathogen *Alternaria brassicicola* induction of b-1,3-glucanase and chitinase activity in the defense response of *Eruca sativa* plants against the fungal pathogen *Alternaria brassicicola*. J. Plant Interact. 8, 155–161. https://doi.org/10.1080/17429145.2012.679705.

Hao, Q., Wang, W., Han, X., Wu, J., Lyu, B., Chen, F., et al., 2018. Isochorismate-based salicylic acid biosynthesis confers basal resistance to Fusarium graminearum in barley. Mol. Plant Pathol. 19, 1995–2010.

Hartman, G.L., Chang, H.X., Leandro, L.F., 2015. Research advances and management of soybean sudden death syndrome. Crop Prot. 73, 60–66. https://doi.org/10.1016/J.CROPRO.2015.01.017.

Hidouri, Safa, Karmous, Inès, Kadri, Oumaima, Kharbech, Oussama, Abdelilah, Chaoui, 2022. Clue of zinc oxide and copper oxide nanoparticles in the remediation of cadmium toxicity in *Phaseolus vulgaris* L. via the modulation of antioxidant and redox systems. Environ. Sci. Pollut. Res. 29 (56), 85271–85285 (accessed 12.28.22). https://link.springer.com/content/pdf/10.1007/s11356-022-21799-2.pdf?pdf=button (accessed 12.28.22).

Ijaz, I., Gilani, E., Nazir, A., Bukhari, A., . Detail review on chemical, physical and green synthesis, classification, characterizations and applications of nanoparticles. http://mc.manuscriptcentral.com/tgcl, 13, pp. 59–81. https://doi.org/10.1080/17518253.2020.1802517.

Inamdar, D.Y., Vaidya, S.R., Mahamuni, S., 2014. On the photoluminescence emission of ZnO nanocrystals, 9, pp. 533–540. https://doi.org/10.1080/17458080.2012.676678.

Iravani, S., 2011. Green Chemistry CRITICAL REVIEW Green synthesis of metal nanoparticles using plants. https://doi.org/10.1039/c1gc15386b.

Ishaq, O. Adisa, Venkata, L. Reddy Pullagurala, Jose, R. Peralta-Videa, Christian, O. Dimkpa, Wade, H. Elmer, Jorge, L. Gardea-Torresdey, Jason, C. White, 2019. Recent advances in nano-enabled fertilizers and pesticides: a critical review of mechanisms of action. Environ. Sci.: Nano 6 (7).

Karmous, I., Gammoudi, N., Chaoui, A., 2022a. Assessing the potential role of zinc oxide nanoparticles for mitigating cadmium toxicity in Capsicum annuum L. under In Vitro Conditions. https://doi.org/10.1007/s00344-022-10579-4.

Karmous, I., Taheur, F.B., Zuverza-Mena, N., Jebahi, S., Vaidya, S., Tlahig, S., Mhadhbi, M., Gorai, M., Raouafi, A., Debara, M., Bouhamda, T., Dimkpa, C.O., 2022b. Phytosynthesis of zinc oxide nanoparticles using *Ceratonia siliqua* L. and evidence of antimicrobial activity. Plants 11, 3079. https://doi.org/10.3390/plants11223079.

Khan, I.H., 2020. Antifungal activity of leaf extract of *Cannabis sativa* against *Aspergillus flavipes* Natural cures for plant diseases View project Cholinesterase inhibitors View project. https://doi.org/10.28941/pjwsr.v26i4.883.

Lanje, A.S., Sharma, S.J., Pode, R.B., Ningthoujam, R.S., 2010. Synthesis and Optical Characterization of Copper Oxide Nanoparticles.

Lefevere, H., Bauters, L., Gheysen, G., 2020. Salicylic acid biosynthesis in plants. Front. Plant Sci. 11, 338. https://doi.org/10.3389/FPLS.2020.00338/BIBTEX.

Leubner-Metzger, G., Meins, F., 1999. Functions and Regulation of Plant ß-1,3-Glucanases (PR-2), pp. 49–76.

Li, S., Wang, Z., Tang, B., Zheng, L., Chen, H., Cui, X., Ge, F., Liu, D., 2021. A pathogenesis-related protein-like gene is involved in the Panax notoginseng defense response to the root rot pathogen. Front. Plant Sci. 11, 2217. https://doi.org/10.3389/FPLS.2020.610176/BIBTEX.

Liu, H., Zheng, S.M., Xiong, H.F., Alwahibi, M.S., Niu, X., 2020. Biosynthesis of copper oxide nanoparticles using *Abies spectabilis* plant extract and analyzing its antinociceptive and anti-inflammatory potency in various mice models. Arab. J. Chem. 13, 6995–7006. https://doi.org/10.1016/J.ARABJC.2020.07.006.

Mali, S.C., Dhaka, A., Githala, C.K., Trivedi, R., 2020. Green synthesis of copper nanoparticles using *Celastrus paniculatus Willd*. Leaf extract and their photocatalytic and antifungal properties. Biotechnol. Rep. 27, e00518 https://doi.org/10.1016/J.BTRE.2020.E00518.

Mazumder, J.A., Khan, E., Perwez, M., Gupta, M., Kumar, S., Raza, K., Sardar, M., 2020. Exposure of biosynthesized nanoscale ZnO to *Brassica juncea* crop plant: morphological, biochemical and molecular aspects. Sci. Rep. 10, 1–13. https://doi.org/10.1038/s41598-020-65271-y.

Naika, H.R., Lingaraju, K., Manjunath, K., Kumar, D., Nagaraju, G., Suresh, D., Nagabhushana, H., 2015. Green synthesis of CuO nanoparticles using *Gloriosa superba* L. extract and their antibacterial activity. Taibah Univ. Sci. 9, 7–12. https://doi.org/10.1016/J.JTUSCI.2014.04.006.

Naseer, M., Aslam, U., Khalid, B., Chen, B., 2020. Green route to synthesize zinc oxide nanoparticles using leaf extracts of *Cassia fistula* and *Melia azadarach* and their antibacterial potential. Sci. Rep. 10, 1–10. https://doi.org/10.1038/s41598-020-65949-3.

Nayan, M.B., Jagadish, K., Abhilash, M.R., Namratha, K., Srikantaswamy, S., 2019. Comparative study on the effects of surface area, conduction band and valence band positions on the photocatalytic activity of ZnO-$M_xO_y$ Heterostructures. J. Water Resour. Prot. 11, 357–370. https://doi.org/10.4236/JWARP.2019.113021.

Niraimathi, K.L., Sudha, V., Lavanya, R., Brindha, P., 2013. Biosynthesis of silver nanoparticles using *Alternanthera sessilis* (Linn.) extract and their antimicrobial, antioxidant activities. Colloids Surf. B: Biointerfaces 102, 288–291. https://doi.org/10.1016/j.colsurfb.2012.08.041.

Omri, K., Najeh, I., Dhahri, R., el Ghoul, J., el Mir, L., 2014. Effects of temperature on the optical and electrical properties of ZnO nanoparticles synthesized by sol-gel method. https://doi.org/10.1016/j.mee.2014.05.029.

Ovais, M., Khalil, A.T., Islam, N.U., Ahmad, I., Ayaz, M., Saravanan, M., Shinwari, Z.K., Mukherjee, S., 2018. Role of plant phytochemicals and microbial enzymes in biosynthesis of metallic nanoparticles. Appl. Microbiol. Biotechnol. 102, 6799–6814. https://doi.org/10.1007/S00253-018-9146-7.

Parveen, K., Banse, V., Ledwani, L., 2016. Green synthesis of nanoparticles: their advantages and disadvantages. AIP Conf. Proc. 1724, 020048 https://doi.org/10.1063/1.4945168.

Patil, S., Chandrasekaran, R., 2020. Biogenic nanoparticles: a comprehensive perspective in synthesis, characterization, application and its challenges. J. Gen. Eng. Biotechnol. 18, 1–23. https://doi.org/10.1186/S43141-020-00081-3.

Peng, S., 2000. Single-leaf and Canopy Photosynthesis of Rice.

Peréz, C.D.P., de La Torre Roche, R., Zuverza-Mena, N., Ma, C., Shen, Y., White, J.C., Pozza, E.A., Pozza, A.A.A., Elmer, W.H., 2020. Metalloid and metal oxide nanoparticles suppress sudden death syndrome of soybean. J. Agric. Food Chem. 68, 77–87. https://doi.org/10.1021/ACS.JAFC.9B06082/SUPPL_FILE/JF9B06082_SI_001.PDF.

Perrot, T., Pauly, M., Plants, V.R., 2022. 2022. Emerging roles of β-Glucanases in plant development and Adaptative responses. mdpi.com. https://doi.org/10.3390/plants11091119.

Pradeep, M., Kruszka, D., Kachlicki, P., Mondal, D., Franklin, G., 2022. Uncovering the phytochemical basis and the mechanism of plant extract-mediated eco-friendly synthesis of silver nanoparticles using ultra-performance liquid chromatography coupled with a photodiode Array and high-resolution mass spectrometry. ACS Sustain. Chem. Eng. 10, 562–571. https://doi.org/10.1021/ACSSUSCHEMENG.1C06960.

Prakash, P., Gnanaprakasam, P., Emmanuel, R., Arokiyaraj, S., Saravanan, M., 2013. Green synthesis of silver nanoparticles from leaf extract of Mimusops elengi, Linn. For enhanced antibacterial activity against multi drug resistant clinical isolates. Colloids Surf. B: Biointerfaces 108, 255–259. https://doi.org/10.1016/J.COLSURFB.2013.03.017.

Ramesh, M., Anbuvannan, M., Viruthagiri, G., 2015. Green synthesis of ZnO nanoparticles using Solanum nigrum leaf extract and their antibacterial activity Spectrochimica Acta part a: molecular and biomolecular spectroscopy. Spectrochim. Acta A Mol. Biomol. Spectrosc. 136, 864–870. https://doi.org/10.1016/j.saa.2014.09.105.

Rastogi, A., Zivcak, M., Sytar, O., Kalaji, H.M., He, X., Mbarki, S., Brestic, M., 2017. Impact of metal and metal oxide nanoparticles on plant: a critical review. Front. Chem. 5, 78. https://doi.org/10.3389/FCHEM.2017.00078/BIBTEX.

Raveendran, P., Fu, J., Wallen, S.L., 2003. Completely "Green" Synthesis and Stabilization of Metal Nanoparticles. https://doi.org/10.1021/ja029267j.

Romadhan, M.F., Suyatma, N.E., Taqi, F.M., 2016. Synthesis of ZnO nanoparticles by precipitation method with their antibacterial effect. journal.ugm.ac.id 16, 117–123.

Rossi, L., Fedenia, L.N., Sharifan, H., Ma, X., Lombardini, L., 2018. Effects of foliar application of zinc sulfate and zinc nanoparticles in coffee (Coffea arabica L.) plants. https://doi.org/10.1016/j.plaphy.2018.12.005.

Ruiz-Herrera, J., Ortiz-Castellanos, L., 2019. Cell wall glucans of fungi. A review. Cell Surface 5. https://doi.org/10.1016/J.TCSW.2019.100022.

Savary, S., Willocquet, L., Pethybridge, S.J., Esker, P., Mcroberts, N., Nelson, A., 2019. The global burden of pathogens and pests on major food crops. https://doi.org/10.1038/s41559-018-0793-y.

Schofs, L., Sparo, M.D., Sánchez Bruni, S.F., 2021. The antimicrobial effect behind Cannabis sativa. Pharmacol. Res. Perspect. 9 https://doi.org/10.1002/PRP2.761.

Segets, D., Gradl, J., Taylor, R.K., Vassilev, V., Peukert, W., 2009. Analysis of optical absorbance spectra for the determination of ZnO nanoparticle size distribution. Solub. Surf. Energy 3, 15. https://doi.org/10.1021/nn900223b.

Sharma, D., Kanchi, S., Bisetty, K., 2019. Biogenic synthesis of nanoparticles: a review. Arab. J. Chem. 12, 3576–3600. https://doi.org/10.1016/J.ARABJC.2015.11.002.

Singh, R.P., Shukla, V.K., Yadav, R.S., Sharma, P.K., Singh, P.K., Pandey, A.C., 2011. Biological approach of zinc oxide nanoparticles formation and its characterization. Adv. Mater. Lett. 2, 313–317. https://doi.org/10.5185/AMLETT.INDIAS.204.

Vert, M., Doi, Y., Hellwich, K.H., Hess, M., Hodge, P., Kubisa, P., Rinaudo, M., Schué, F., 2012. Terminology for biorelated polymers and applications (IUPAC recommendations 2012). Pure Appl. Chem. 84, 377–410. https://doi.org/10.1351/PAC-REC-10-12-04/PDF.

Wang, Y., Zhang, C., Bi, S., Luo, G., 2010. Preparation of ZnO nanoparticles using the direct precipitation method in a membrane dispersion micro-structured reactor. https://doi.org/10.1016/j.powtec.2010.04.027.

Wu, J., Kim, S.G., Kang, K.Y., Kim, J.G., Park, S.R., Gupta, R., Kim, Y.H., Wang, Y., Kim, S.T., 2016. Overexpression of a pathogenesis-related protein 10 enhances biotic and abiotic stress tolerance in Rice. Plant Pathol. J. 32, 552–562. https://doi.org/10.5423/PPJ.OA.06.2016.0141.

Zafar, H., Ali, A., Ali, J.S., Haq, I.U., Zia, M., 2016. Effect of ZnO nanoparticles on *Brassica nigra* seedlings and stem explants: growth dynamics and antioxidative response. Front. Plant Sci. 7, 535. https://doi.org/10.3389/FPLS.2016.00535/BIBTEX.

Zhang, S.B., Zhang, W.J., Zhai, H.C., Lv, Y.Y., Cai, J.P., Jia, F., Wang, J.S., Hu, Y., 2019. Expression of a wheat β-1,3-glucanase in *Pichia pastoris* and its inhibitory effect on fungi commonly associated with wheat kernel. Protein Expr. Purif. 154, 134–139. https://doi.org/10.1016/J.PEP.2018.10.011.

Zimniewska, M., Pawlaczyk, M., Romanowska, B., Gryszczyńska, A., Kwiatkowska, E., Przybylska, P., 2021. Bioactive hemp clothing modified with cannabidiol (Cbd) *cannabis sativa* l. extract. Materials 14. https://doi.org/10.3390/MA14206031.

Zubrod, J.P., Bundschuh, M., Arts, G., Brühl, C.A., Imfeld, G., Knäbel, A., Payraudeau, S., Rasmussen, J.J., Rohr, J., Scharmüller, A., Smalling, K., Stehle, S., Schulz, R., Schäfer, R.B., 2019. Fungicides: an overlooked pesticide class? Environ. Sci. Technol. 53, 3347–3365. https://doi.org/10.1021/ACS.EST.8B04392/ASSET/IMAGES/LARGE/ES-2018-04392F_0005.JPEG.

Sheteiwy, M.S., Shaghaleh, H., Yousef, Hamoud A., Holford, P., Shao, H., Qi, W., Hashmi, Z., Wu, T., 2021. Zinc oxide nanoparticles: potential effects on soil properties, crop production, food processing, and food quality. Environ. Sci. Pollut. Res. Int. 28 (28), 36942–36966. https://doi.org/10.1007/s11356-021-14542-w/Published.